PRODUCTION OF SYNGAS VIA GLYCEROL BIOMASS USING LIMESTONE BASED CATALYST

by

Do Minh Tuan

Dissertation submitted in partial fulfilment of
the requirements for the
Bachelor of Engineering (Hons)
(Chemical Engineering)

December 2012

Universiti Teknologi PETRONAS
Bandar Seri Iskandar
31750 Tronoh
Perak Darul Ridzuan

CERTIFICATION OF APPROVAL

PRODUCTION OF SYNGAS VIA GLYCEROL BIOMASS USING LIMESTONE BASED CATALYST

by

Do Minh Tuan

A project dissertation submitted to the
Chemical Engineering Programme
Universiti Teknologi PETRONAS
in partial fulfilment of the requirements for the
BACHELOR OF ENGINEERING (Hons)
(CHEMICAL ENGINEERING)

Approved by,

_____

(Dr. Bawadi B Abdullah)

UNIVERSITI TEKNOLOGI PETRONAS

TRONOH, PERAK

December 2012

CERTIFICATION OF ORIGINALITY

This is to certify that I am solely responsible for the work submitted in this project, that the original work is my own except as specified in the references and acknowledgements, and that the original work contained herein have not been undertaken or done by unspecified sources or persons.

_____

DO MINH TUAN

ABSTRACT

The mass production of biodiesel nowadays has produced surplus of glycerol as glycerol is a by-product of biodiesel processing. This would decrease the price market of glycerol as the conventional applications and current market cannot cope with this rate of production. As Malaysia is among the top producer of glycerol, it will cause some negative effects on the country. The main objective of this project is to investigate the potential of syngas production via glycerol using limestone based catalyst utilizing dry reforming technique. In the beginning, the limestone based catalyst is characterized by using TGA, TEM and BET analysis to determine the calcination temperatures, composition, arrangement and surface area size. After limestone characterization, the catalyst is prepared using impregnation of limestone support with metal precursor solution, followed by drying and calcination. The catalysts would be characterized again using TEM and BET method to determine the composition and specific size range of catalyst particle in order to compare the differences before and after catalyst preparation. Finally, the reaction will be carried out in a fixed bed reactor loading of catalyst in the middle with glycerol and CO_2 as the reactants input with the flow rate of 3mL/min and 100mL/min, respectively in an operating temperature of 500^{o}C under various operating pressure. This project is proven to be successful by the fact that all of the three $CaCO_3$ and CaO based catalysts have the capability to transform glycerol into syngas via dry reforming reaction with H_2 concentration ranges from 40 to 87% of molar concentration while CO concentration has the range of 0.36 to 7%. Moreover, it is observed that the H_2/CO ratio yields are directly proportional to the operating pressure of the reactor. These results have shown some potential promises which would in turn create a big opportunity for Malaysia to convert glycerol into high value product syngas as limestone and glycerol are abundance in the country. Further researches and projects would be recommended to enhance the conversion and selectivity as well as developing new method and techniques such as steam reforming and pyrolysis to carry out the process in bigger scales.

ACKNOWLEDGEMENT

First and foremost, I would like to express my sincere gratitude and appreciation to my supervisor, Dr. Bawadi Bin Abdullah for his invaluable advice, support, encouragement, and his patience throughout this course of my project. I am forever grateful to him for believing in me and giving me the opportunity to work with him, and being such an inspiring mentor with his immense enthusiasm.

I am also greatly thankful to Assoc. Prof. Dr. Suzana Yusup for her generous help, her expert advice, and her support to me like as if I am one of her own students. I would also like to express my appreciation to Prof. Dr. Yoshimitsu Uemura, who has generously given me all the necessarily support at the end of my project.

Moreover, I would like to express my gratitude to the two Post Graduate students, Mr. Farrukh and Ms. Hafizah who have contributed to my project with directional guidance, constructive feedbacks as well as instructions in order for me to successfully complete my project.

Last but not least, I would like to express my true appreciation to my parents and family for their love, emotional support, understanding, moral as well as physical supports. Not forgetting on how they spare their valuable time and sponsorship to ensure the success of this project.

To all individuals who helped me directly or indirectly, but whose name was not mentioned here, I would like to thank you all.

CONTENTS

ABSTRACT…… i

ACKNOWLEDGEMENT……..……ii

1 INTRODUCTION 1

2 LITERATURE REVIEW 3

2.1 Glycerol 3

2.2 Limestone 3

2.3 Syngas 4

2.4 Reforming in supercritical water 4

2.5 Pyrolysis 5

2.6 Dry reforming 5

2.7 Potential of limestone as the based catalyst 6

3 METHODOLOGY 8

3.1 Methodology Flowchart 8

3.2 Thermogravimetric Analysis (TGA) 10

3.3 Transmission Electron Microscopy (TEM) 11

3.4 BET Adsorption Method 12

3.5 Preparation of catalyst 14

3.5.1 Impregnation 15

3.5.2 Drying 17

3.5.3 Calcination 17

3.5.4 Reduction 18

3.6 Experiment 19

3.6.1 Experimental setup 20

3.6.2 Design of Experiments 21

4 RESULTS AND DISCUSSION 23

4.1 Catalyst Characterization 23
4.2 Experimental Results 27
5 CONCLUSIONS AND RECOMMENDATIONS 32
5.1 Conclusion 32
5.2 Recommendations 33
6 REFERENCES 34
7 APPENDICES 36

LIST OF FIGURES

Figure 3.1: Methodology Flow Chart 8
Figure 3.2: BET plot 13
Figure 3.3: Catalyst Preparation Steps 14
Figure 3.4: Reactor configurations 20
Figure 4.1: Three Catalysts Sample 23
Figure 4.2: TEM images of $CaCO_3$ and $NiO/CaCO_3$ after calcination 25
Figure 4.3: TEM images of $CaCO_3$ and $ZnO/CaCO_3$ after calcination 25
Figure 4.4: TEM images of CaO and ZnO/CaO after calcination 26
Figure 4.5: Air Bags Product Sample 27
Figure 4.6: Reference calibration curve of Shimadzu GC 28

LIST OF TABLES & GRAPHS

Table 3.1: Amount of metal precursor and support 16
Table 3.2: pH of Catalysts..... 17
Table 3.3: Design of Experiments..... 21
Table 4.1: BET Results 23
Table 4.2: Retention time of main components 30

Graph 3.1: Thermal decomposition curve of Calcium Carbonate 10
Graph 4.1: Viscosity of common carrier gases 29
Graph 4.2: Relationship between types of catalysts and operating pressure towards H_2/CO Ratio 30

LIST OF ABBREVIATIONS

CAL: Central Analytical Laboratory

CBBR: Centre of Bio-Fuel and Bio-Chemical Research

FYP: Final Year Project

GC: Gas Chromatography

TEM: Transmission Electron Microscopy

TGA: Thermogravimetric Analysis

1 INTRODUCTION

Nowadays, fossil fuel is being used widely as one of the major energy sources to fulfill our energy requirements. However, this resource is depleting fast and considered as a source of global warming (Norhasyimi, Ahmad, & Abdul, 2010). Numerous alternative fuels such as hydrogen, biodiesel and ethanol are being produced and applied in various fields to meet our energy demand. In the world, biodiesel production rate is increasing every year to sustain the energy needs. Even in Malaysia, the production of biodiesel is announced as 500,000 tons per year and the government hopes to increase this number every year (Norhasyimi et al., 2010). During the production of biodiesel, glycerol can be obtained as a by-product. The mass production of biodiesel indicated that the glycerol production would be increasing as well. As the current ordinary applications and market demand cannot cope with the surplus of glycerol, a decrease in glycerol market price is inevitable. Moreover, as Malaysia is among the major producer of glycerol derived from palm oil, this problem would have a negative effect on the country. To overcome this coming problem, several researches and efforts have been considerably developed and continuously investigated to transform the low value glycerol by utilizing different approaches and strategies.

The main objective of this FYP project is to investigate the potential of syngas production via glycerol using limestone based catalyst by utilizing dry reforming technology. The dry reforming of glycerol reactions will be carried out in a fixed-bed reactor with limestone based catalyst. The effects of CO_2 flow rate, temperature and characteristics of limestone based catalyst on the product yield, product gas compositions, glycerol conversion will be studied to demonstrate the possibilities of this new technique.

Although the production of syngas by using glycerol as the feedstock have been developed using different methods before, none of these has utilized limestone as the

based catalyst. Therefore, this project, if proved to be successful, is more applicable to Malaysia and can contribute a great deal towards the development of syngas production in the country due to the abundance and inexpensive price of the two main process inputs: glycerol and limestone.

2 LITERATURE REVIEW

2.1 Glycerol

Glycerol is the simplest trihydric alcohol which has IUPAC name of propane-1,2,3-triol. It can be called as glycerin, 1,2,3-propanetriol, 1,2,3-trihydroxypropane, glyceritol or glycyl alcohol. Pure glycerol appears as a colourless, odourless, viscous liquid with syrupy and sweet taste. Glycerol can be used in various applications such as pharmaceutical, chemical intermediate and food. Norhasyimi et al. (2010) also reported that glycerol can be converted to more valuable product via selective oxidation, hydrogenolysis, dehydration, selective oligomerization, reforming towards syngas, esterification and etherification.

Glycerol appears to be a potential feedstock to be used in the production of syngas since Malaysia is among the top worldwide producer of glycerol which derived from the production of biodiesel from palm oil. Moreover, in Malaysia, biodiesel production has been announced as 500,000 tonnes per year and the government hopes to increase this number every year (Norhasyimi et al., 2010). As glycerol is a by-product obtained during the production of biodiesel, it will lead to an entail surplus of glycerol production. Therefore, the conventional applications and current market of glycerol could not cope with the availability of glycerol which would likely to reduce the price of glycerol feedstock negatively. To avoid this problem, it is necessary to find a way to produce glycerol into useful product such as syngas.

2.2 Limestone

Limestone is a sedimentary rock consisting mainly of the mineral calcite (calcium carbonate, $CaCO_3$) and another common mineral which is dolomite [$CaMg(CO_3)_2$]. Common impurities in limestone include chert (microcrystalline, cryptocrystalline quartz or amorphous silica, SiO_2), clay, organic matter and iron oxides. Tan (1998) stated that limestone is abundance in Malaysia, occurring in the forms of numerous limestone hills and bedrocks. Therefore, if limestone is proved successfully to be the

based catalyst for syngas production, it would be the most efficient and effectively based catalyst due to its availability in Malaysia.

2.3 Syngas

Syngas or synthesis gas, is a gas mixture that contains varying amounts of carbon monoxide and hydrogen and very often, an infinitesimal amount of carbon dioxide. Syngas can be used as an intermediate in producing synthetic natural gas or to create ammonia or ethanol and other synthetic petroleum. The process of transforming glycerol into syngas by using different techniques has been carried out before: hydrogen production from glycerol by reforming in supercritical water over Ru/Al_2O_3 catalyst (Adam, Pant, & Ram, 2008), pyrolysis of glycerol for the production of hydrogen or syngas (Valliyapan, Bakhshi, & Dalai, 2007), syngas from steam reforming of glycerol using platinum catalyst (Francisco, 2010) and dry reforming of glycerol for syngas production (Fernandez, Arenillas, Bermudez, & Menendez, 2010).

2.4 Reforming in supercritical water

Adam et al. (2008) carried out hydrogen production from glycerol by supercritical water reforming over Ru/Al_2O_3 catalyst in a tubular fixed-bed flow reactor. In the experiments, the results were reported that supercritical reforming of glycerol produced a stream rich in H_2 and CO_2 with a small amounts of CH_4 and CO and the conversion of glycerol was always greater than 99% with short residence time and operating temperature at 800^oC. They suggested that the reforming of glycerol for hydrogen production can be summarized with these reactions:

Steam reforming of glycerol: $C_3H_8O_3 \rightarrow 3CO+4H_2$

Water gas shift reaction: $CO+H_2O \rightarrow CO_2+ H_2$

Overall reaction: $C_3H_8O_{3+}\ 3H_2O \rightarrow 3CO_2+7H_2$

Some hydrogen will be lost to produce CH_4 via the methanation of CO and CO_2:

$CO+3H_2 \rightarrow CH_4+ H_2O$

$CO_2+4H_2 \rightarrow CH_4+ 2H_2O$

2.5 Pyrolysis

The pyrolysis of glycerol to produce syngas with nitrogen as the carrier gas was done by Valliyapan et al. (2007) suggested that a large amount of syngas of 93.5 mol% would be produced with operating temperature at 800^oC. Moreover, it is reported by Wang et al (1996) that the pyrolysis process involves several parallel reactions to produce a small amount of methane, carbon dioxide and coke with the following reaction:

$C_mH_nO_k \rightarrow C_xH_yO_z+$ gas (H_2, CO, CH_4, CO_2…) + Coke

2.6 Dry reforming

Although production of syngas by glycerol pyrolysis and steam reforming have been applied and analyzed in details, little information is available for dry reforming. Xiaodong et al (2009) have carried out researches to investigate the possibility of glycerol dry reforming for syngas production using total Gibbs free energy minimization method. Their conclusion is that with a temperature of 700K and CO_2 to glycerol ratio of 1, we can achieve maximum syngas production with H_2: CO=1:1 and the conversion of CO_2 is 33%. They have suggested these main reactions for dry reforming:

$C_3H_8O_3 \Leftrightarrow 3\ CO+4H_2$

$CO+3H_2 \Leftrightarrow CH_4+ H_2O$

$CO_2+4H_2 \Leftrightarrow CH_4+ 2H_2O$

$$CO_2 + CH_4 \Leftrightarrow 2CO+2H_2$$

$$CO + H_2O \Leftrightarrow CO_2+H_2$$

$$C+ H_2O \Leftrightarrow CO+ H_2$$

$$CH_4 \Leftrightarrow 2H_2 + C$$

$$2CO \Leftrightarrow CO_2 +C$$

$$C+ 2H_2O \Leftrightarrow CO_2+2H_2$$

2.7 Potential of limestone as the based catalyst

Fernandez et al (2010) has shown that carbon based catalysts seems to be ideal for producing syngas with the ratio of H_2/CO close to 1 with a very minimal CO_2 emission. Moreover, they also reported that in syngas production using steam reforming with carbonaceous catalyst, as water to glycerol molar ratio increases, the conversion of glycerol to gaseous product decreases. Finally, by comparing the three methods of producing syngas via three different processes: pyrolysis, steam reforming and dry reforming on the same carbon based catalyst, they concluded that by using glycerol feed as reference, the steam reforming experiments produced the highest syngas and H_2 yield compared to other two processes.

In preparation of the limestone based catalyst, the impregnation method, followed by drying and calcination have been applied in recent preparation of limestone support catalyst for transesterification of vegetable oils, carried out by Chawalit et al (2011). Before the preparation steps, the based catalyst has been characterized using these methods: Transmission Electron Microscope (TEM) for morphological study, BET analysis for the calculation of surface area and finally Thermogravimetric analysis (TGA) to establish the thermal decomposition profile of the based catalyst. Thus, the methods that we have chosen to prepare the catalyst should follow this procedure: limestone calcination temperature check by using TGA, the next step is impregnation which is performed with the solution of Nickel Nitrate $Ni(NO_3)_2.6H_2O$ and Zinc Nitrate $Zn(NO_3)_2.6H_2O$, and subsequently, drying and calcination of the catalyst.

From the literature review above, it is possible that glycerol- which is easy to be found in Malaysia can possibly be used as a feedstock to produce syngas through these possible processes: pyrolysis, supercritical water reforming, and catalytic steam reforming or dry reforming. As stated in the title, we are planning to use limestone as the based catalyst for this process since limestone consists mainly of $CaCO_3$ which can be considered as a suitable carbonaceous catalyst since it contains carbonate ions CO_3^{2-}. Therefore, this project, if proved to be successful, can contribute a great deal to the development of syngas production in Malaysia by utilizing two available and abundance process inputs: glycerol and limestone.

3 METHODOLOGY

3.1 Methodology Flowchart

The flowchart below has clearly summarised all the important steps in the methodology of this project:

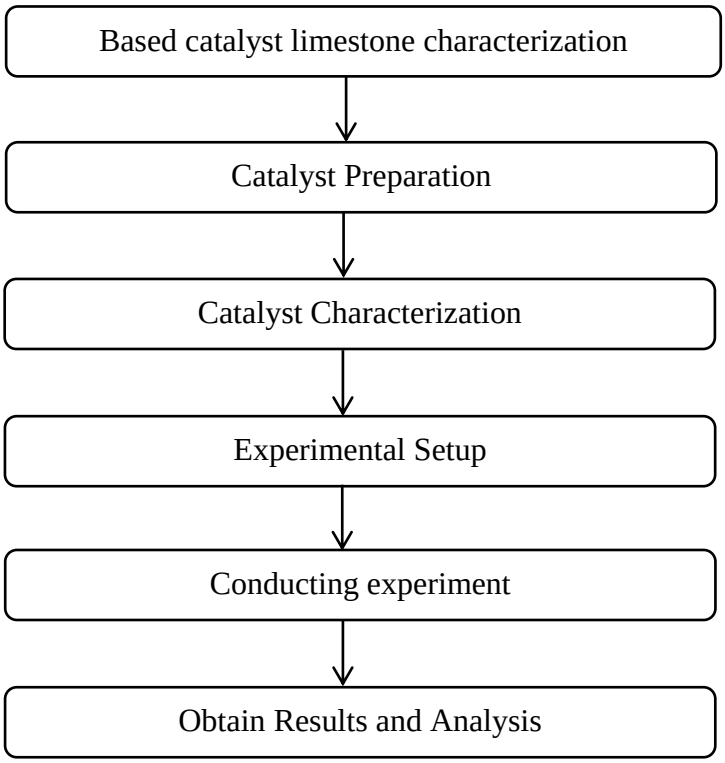

Figure 3.1: Methodology Flow Chart

In my experiment, due to the unavailability of limestone feedstock, Calcium Carbonate $CaCO_3$ and Calcium Oxide CaO have been used as the support since limestone consists mainly of $CaCO_3$. Moreover, as the experiment carried out by Fernandez et al. (2010) has shown that carbon based catalysts seem to be ideal for producing syngas. At first, the $CaCO_3$ and CaO must have been characterized using the following procedures: Thermogravimetric Analysis (TGA) to determine the suitable calcination temperature, BET analysis and TEM (Transmission Electron Microscopy) to examine the surface area and pore sizes. After the calcination step, the catalyst powder would be analysed by using two of the following procedures:

BET analysis and TEM to compare the differences of the surface area and pore sizes before and after catalyst preparation.

From the justifications above, 3 types of catalysts have been prepared in this experiment: $Zn/CaCO_3$, Zn/CaO and $Ni/CaCO_3$. Since Bournay et al. (2005) has stated that Axens has successfully commercialized the first heterogeneously catalyzed biodiesel production process using mixed oxide of Zinc (Zn) and Alumina (Al) as the catalyst solid base, I have decided to choose Zn as the metal precursor and Ni is selected to be the second option metal precursor because Ni shows some potential promises in converting glycerol into syngas according to Xiaodong et al. (2009).

3.2 Thermogravimetric Analysis (TGA)

The purpose of Thermogravimetric Analysis is to perform an analysis of thermal decomposition of $CaCO_3$ in a controlled atmosphere by recording the mass of the $CaCO_3$ sample as a function of temperature or time as the temperature of the sample is increased.

Below is the graph of the thermal decomposition of our $CaCO_3$ sample, analysed by the laboratory. In this graph, the temperature is programmed to increase from 20°C to 900°C with the rate of 25°C/ minute in nitrogen atmosphere:

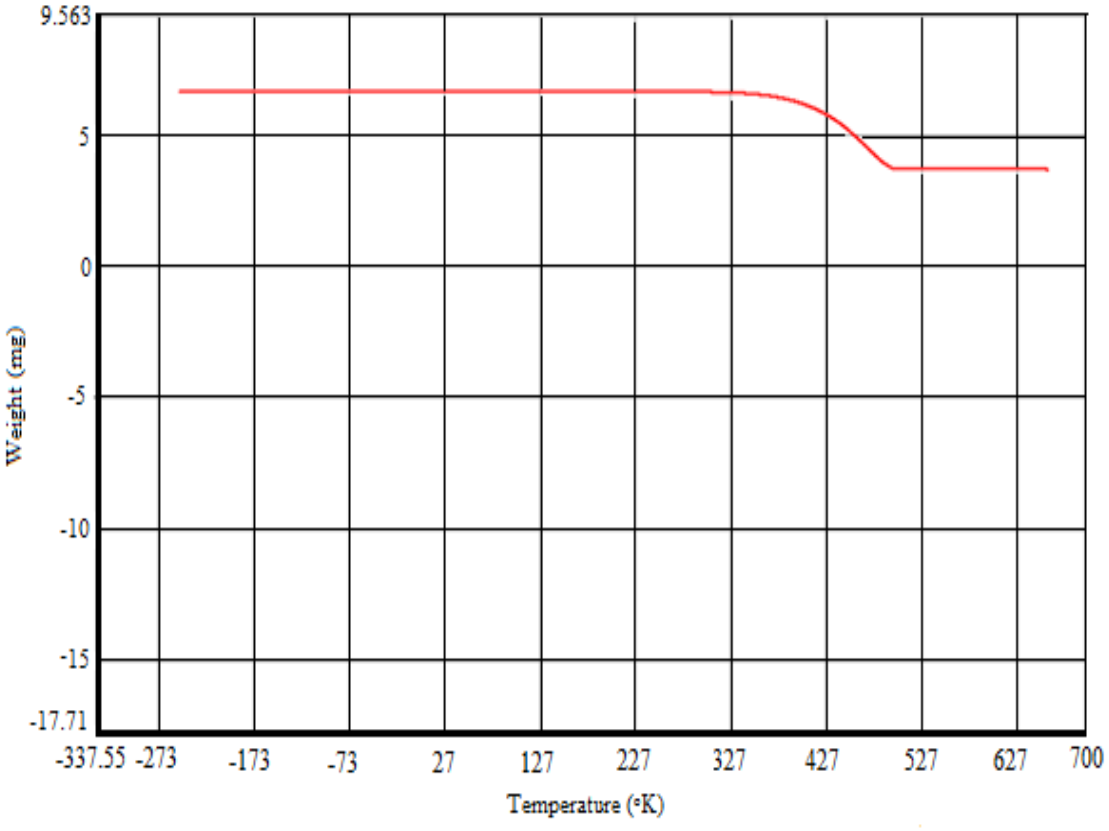

Graph 3.1: Thermal decomposition curve of Calcium Carbonate

From this graph, the temperature of the transition from calcium carbonate ($CaCO_3$) into calcium oxide (CaO) is predicted as $CaCO_3$ decomposes into CaO as the temperature increases by the following reaction:

$$CaCO_3\,(s) \xrightarrow{650^{o}C} CaO\,(s) + CO_2\,(g)$$

Therefore, with the thermal decomposition curve obtained, only one calcination temperatures would be chosen to prepare the samples as well as to satisfy the reaction operating temperature. By looking at the graph, we can see that the $CaCO_3$ sample begins to decompose to CaO at a temperature higher than $650^{o}C$. Therefore, the temperature of calcination has been chosen at $600^{o}C$ in order to calcine the catalyst with $CaCO_3$/CaO support without decomposing $CaCO_3$.

3.3 Transmission Electron Microscopy (TEM)

After this step, TEM is performed to examine the surface of the three catalyst samples. TEM equipment is designed to transmit a beam of electron through the sample, resulting in the interaction between the beam of electrons and the electrons of the sample itself. This would lead to the scattering of electrons which are diffracted in a certain order based on the organization of the powder structures. The results will be obtained by forming an image on an imaging device which can be magnified to observe the arrangement and spacing of atoms. The results from TEM analysis would be supported by BET analysis to determine the size of the average particles and the specific range of the particle sizes.

3.4 BET Adsorption Method

Finally, the BET Adsorption is followed to measure the specific area and pore volume of the three samples. According to Pomonis et al (2005), the BET method is primarily based on the BET equation which is an extension of the Langmuir theory:

$$\frac{V}{V_m} = \frac{CP}{[1 + (C - 1)P][1 - P]}$$

V: adsorbed gas quantity.

V_m: monolayer adsorbed gas quantity.

P: equilibrium pressure of adsorbates at the temperature of adsorption.

C: BET constant.

By plotting P [V(1-P)] vs P, we can obtain V_m and C using these formulas:

$$V_m = \frac{1}{A+I}$$

$$C = 1 + \frac{A}{I}$$

A and I are the slope and intercept of the graph which is illustrated below:

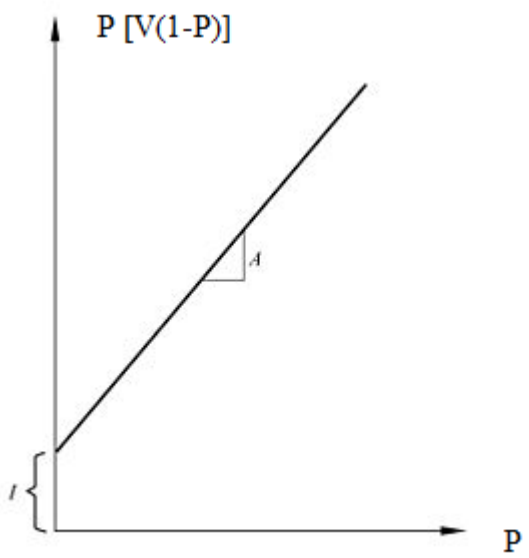

Figure 3.2: BET plot

From V_m and C, the total surface area S_{Total} and the specific surface area S_{BET} are evaluated using the equations:

$$S_{Total} = \frac{Vm.N.s}{v}$$

$$S_{BET} = \frac{S_{Total}}{a}$$

N: Avogadro's number

s: adsorption cross section of the adsorbing species.

v: molar volume of adsorbate gases.

a: mass of adsorbent (in gram).

As a result, the BET methods will help us to fully evaluate the specific and total surface area as well as the volume of the pores of the three calcite limestone samples.

3.5 Preparation of catalyst

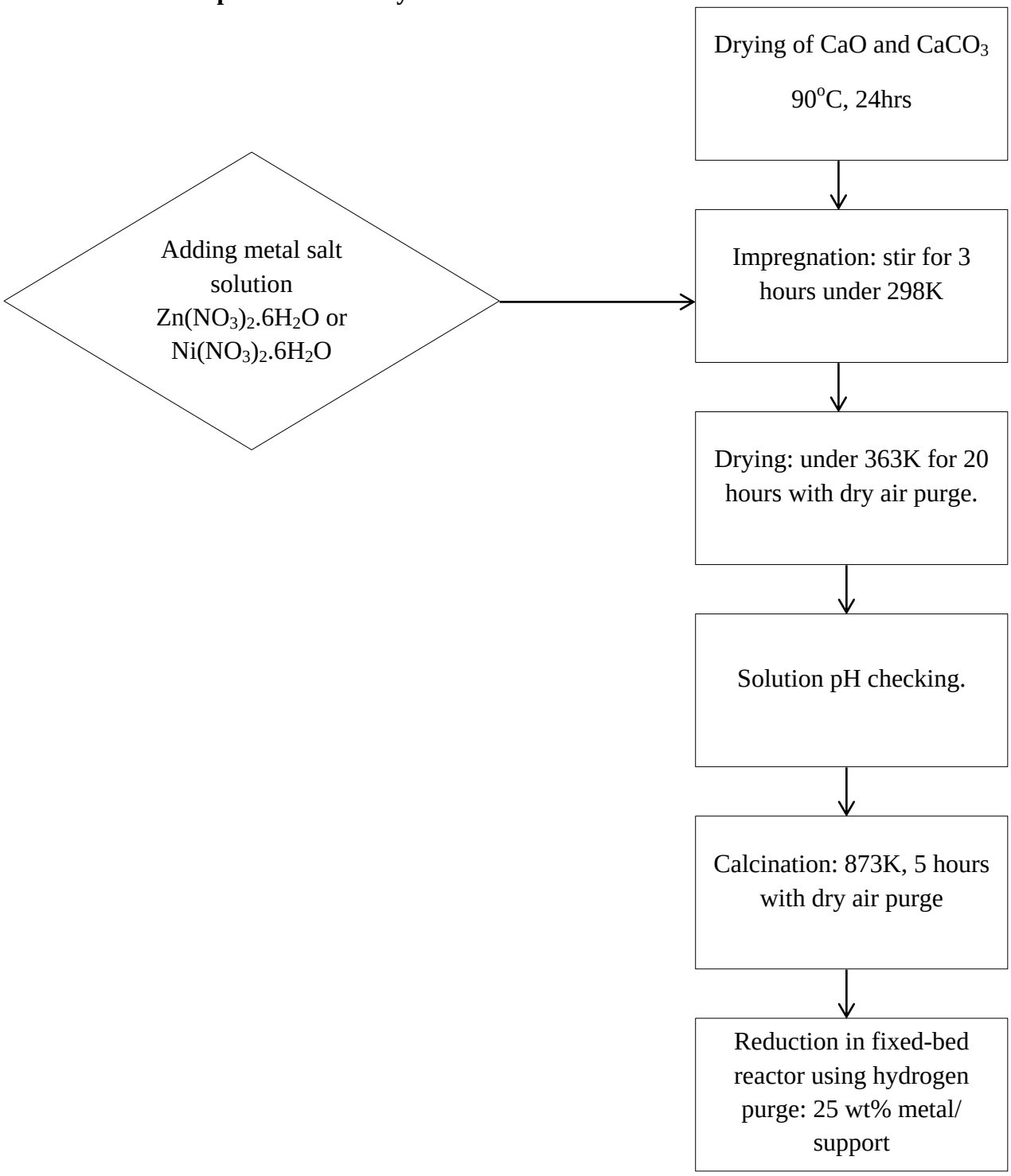

Figure 3.3: Catalyst Preparation Steps

In the catalyst preparation, I have successfully produced 3 types of catalyst: Zn/ $CaCO_3$, Zn/CaO and Ni/ $CaCO_3$. The 3 types of catalyst have been ready until the calcination step where the metal precursors are existed in oxide form. The procedure for the catalyst preparation are summarised below.

3.5.1 Impregnation

Until this point, we are required to choose either one of the two methods of impregnation (Francesco, 1998) depends upon the characteristic of each sample of limestone: incipient wetness or wet impregnation. In incipient wetness method (dry impregnation), the impregnating solution would be sprayed on the surface of the $CaCO_3$ based catalyst in a way that the solution does not exceed the pore volume of the support. However, wet impregnation involves the wet mixing of limestone powder with the solution of the metal precursor. This technique involves the use of metal precursor solution in excess compared to the pore volume of $CaCO_3$ as the support base. The $CaCO_3$ will be immersed in the metal solution.

Using the CaO support with $Zn(NO_3)_2.6H_2O$ as an example, by applying the wet impregnation method, the CaO will be loaded into a beaker with an amount of 17 gram. The solution of $Zn(NO_3)_2.6H_2O$ is pour into the beaker with an amount of 19 gram. The amount of activated metal Zn in the catalyst can be calculated by using the following formula:

$$m_{Zn}= \frac{19*\text{Molecular weight of Zn}}{\text{Molecular weight of Zn(NO3)2.6H2O}} = \frac{19*65.4}{297.48}=4.17 \text{ (gram)}$$

Thus, the final loading of catalyst is estimated to be 23.5% weight with 4 gram of Zn: 17 gram of CaO. 50mL of water is added to set up the concentration of Zn solution to be 0.08 gram/mL.

The table below summarised the amount of $Zn(NO_3)_2.6H_2O$ and $Ni(NO_3)_2.6H_2O$ used and the metal loading for the catalysts:

Catalyst	Zn/ $CaCO_3$	Zn/CaO	Ni/$CaCO_3$
Weight metal/support	4g Zn: 17g $CaCO_3$	4g Zn: 17g $CaCO_3$	4g Ni: 16g $CaCO_3$
Amount of metal solution	19g of $Zn(NO_3)_2.6H_2O$	19g of $Zn(NO_3)_2.6H_2O$	19.7g of $Ni(NO_3)_2.6H_2O$

Table 3.1: Amount of metal precursor and support

The next step of impregnation is to stir the solution using a magnetic stirrer for consecutively 3 hours under ambient pressure with a small amount of heat applied to remove excess water. After this step, the solution now will be checked for pH by using the pH meter before entering the oven for drying. The purpose of pH checking is to determine whether the surface of the catalyst support will adsorb anions or cations during the catalyst preparation process.

Reasons to check for pH:

According to Francesco (1998), in acidic solution, the surface of the support is positively charged and thus, covered with anions while in the opposite, in a basic solution, the surface of the support is negatively charged and covered with cations. For each metal oxide, at a given pH, the surface charge is equal to zero which is called PZC (zero point of charge) or IEPS (isoelectric point). The PZC of NiO is 10-11 pH (8.7-9.7 for ZnO) which means that with a pH above 11, the surface of the support with NiO will be negatively polarized and will adsorb cations. In contrast, the surface of the support will be positively charged and covered with anions if the pH is below 10.

Here is the summarized table pH of the three catalyst solutions:

Catalyst	Zn/ $CaCO_3$	Zn/CaO	Ni/$CaCO_3$
pH measured	6.1	11.79	8.06
PZC	8.7-9.7	8.7-9.7	10-11
Characteristic	Positively polarized	Negatively polarized	Positively polarized

Table 3.2: pH of Catalysts

3.5.2 Drying

The catalyst solution now is dried in the oven typically under 90^{o}C for 20 hours continuously. The solution is stirred for three times at the first three hours. The purpose of drying is to eliminate the solvent that has been used in the previous impregnation step (water for my case). In the drying step, I have successfully maintained the drying at 90^{o}C to make sure the catalyst will be distributed uniformly. The reason is that if the drying rate is too slow, the evaporation of water at the surface will diffuse the salt deeper into the liquid in the pore which would lead to high concentration of solution in the pore. At the precipitation step, the metal precursor will mainly concentrate at the bottom of the pore. In contrast, if the drying rate is too fast, the metal precursor will be forced to the outer layer of the particles. After the drying step, the catalyst, now in solid form, is crunched into pellets.

3.5.3 Calcination

The catalyst is now transferred to a crucible to undergo through the calcination step. Calcination process involves heating the catalyst in an oxidizing atmosphere to decompose the metal precursor and removal of gaseous product. In this case, the treatment is used to form the metal oxide of Ni (NiO) and at the same time, removing the gaseous product NO_2 and O_2 by the following reactions:

$$Zn\,(NO_3)_2 \rightarrow ZnO + 2NO_2 + \frac{1}{2}O_2$$

$$Ni\,(NO_3)_2 \rightarrow NiO + 2NO_2 + \frac{1}{2}O_2$$

This is typically carried out under the temperature as high as or a little higher than the temperature during the later reaction (in my case because my experiment is required to carry out at 500^{o}C then the operating temperature of the furnace has been chosen to be 600^{o}C). This calcination process takes roughly 5 hours and requires purging air to continuously remove the gaseous product as NO_2 is a combustible substance which may cause explosion hazards under high temperature in the furnace.

3.5.4 Reduction

The metal oxide catalyst $ZnO/CaCO_3$ is transformed into $Zn/CaCO_3$ by thermal treatment in hydrogen flow to completely remove the oxide. The reduction gas hydrogen must contain water vapour as low as possible to prevent the bad effects to the dispersion of the metal on the catalyst support. Moreover, the rate of hydrogen has to be high enough to remove the water formed during the reduction from the catalyst support. During this thermal treatment, the reduction temperature has been chosen as 500^{o}C and the flow rate of hydrogen as 10mL/min for 1 hour continuously. However, in this case, nitrogen, which is an inert gas, is also supplied simultaneously as 50mL/min to dilute the hydrogen in order to reduce the risk of hydrogen explosion.

The reduction step will be carried out right before the dry reforming reaction between glycerol and CO_2 by loading the catalyst inside the reactor and let hydrogen flow through. With this, we can immediately run the reaction with glycerol after the catalyst has been reduced in the reactor.

3.6 Experiment

The next step is to conduct the experiment to transform glycerol into syngas. The catalyst will be located inside a fixed bed reactor with CO_2 and glycerol as the inputs. As we are doing the dry reforming reactions of glycerol, the optimized conditions proposed by Xiaodong et al. (2009) would be followed as: CO_2 and glycerol will be supplied with CO_2 to glycerol ratio of 0.5 to 1 under operating temperature at 500^oC and atmospheric pressure.

Although the steam reforming technique has shown several advantages over pyrolysis and dry reforming, the main reason why we want to perform dry reforming is that glycerol dry reforming will convert CO_2 into synthesis gas and remove it from the carbon biosphere cycle. It will be beneficial to the environment compared to other two processes. Therefore, this dry reforming of glycerol experiment will carry out two duties at the same time: transform glycerol into high value product: syngas as well as reducing the green-house effects.

3.6.1 Experimental setup

The experiment is conducted as suggested by Eigenberger (2000) which can be simplified below:

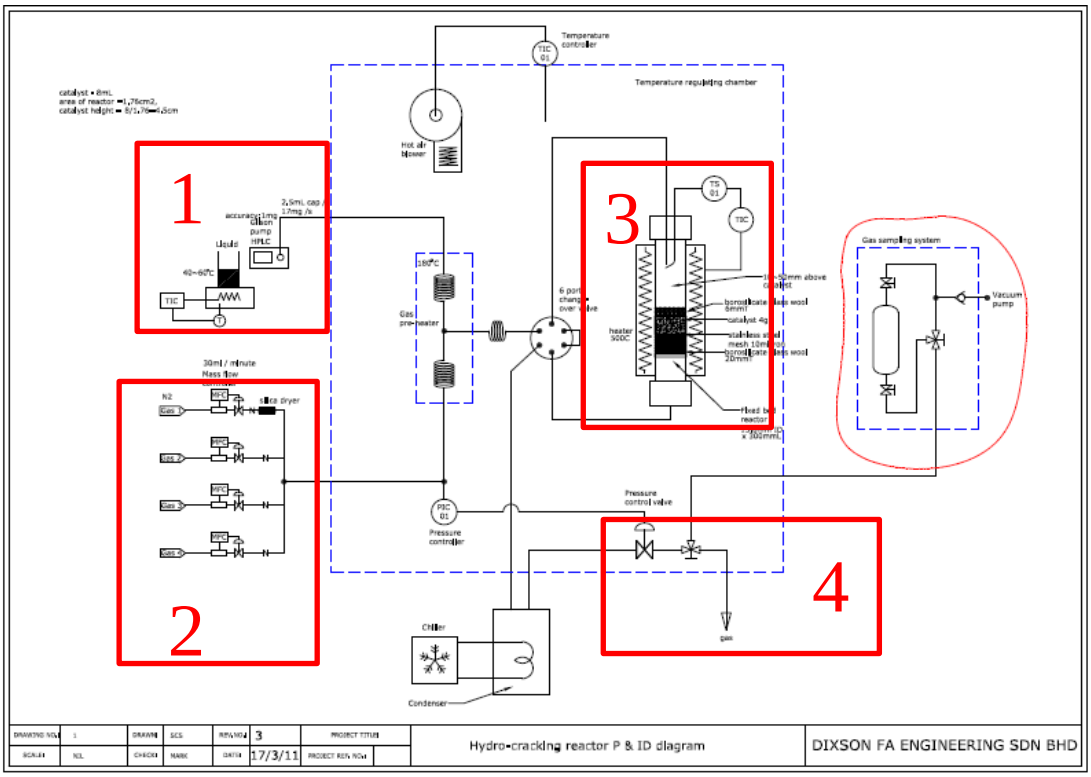

1: Glycerol pump

2: Flow Controller of CO_2

3: Fixed Bed Reactor

4: Sampling Cylinder

Figure 3.4: Reactor configurations

This reactor, which is located in CBBR, is a fixed bed reactor which the catalyst is loaded at the middle between two layers of glass wool and mesh. The reactor is designed as a cylinder with 15.6mm inner diameter and 300mm in length, covered by a heater along the whole body. The complete configurations of the reactor can be observed in Appendix A. First of all, right after the reduction of catalyst, the glycerol will be supplied to the reactor using the pump. Before reaching the core of the reactor, glycerol is pre-heated to 300^{o}C by a hot air blower located at the top of the reactor to completely transform glycerol into vapour. At the same time, CO_2 is supplied through the gas flow controller. These two gases react with each other over the surface of the limestone based catalyst under operating conditions of 500^{o}C and atmospheric pressure. The gaseous products will be collected at the gas sampling system. After the pressure in the reactor exceeds the set point pressure of the pressure control valve, the product will be pumping by the vacuum pump to the sampling cylinder at the bottom of the reactor. These gases will be transferred to the air bags by connecting to an external line. There are nine air bags collected according to nine different operating conditions, which is shown in the design of experiment below.

3.6.2 Design of Experiments

Run	Type of Catalyst	Temperature (˚C)	Catalyst to Glycerol Ratio (Weight Ratio)	Carbon Dioxide Flow Rate (ml/min)	Pressure (atm)
1	$Zn/CaCO_3$	500	2:30	100	1
2	$Zn/CaCO_3$	500	2:30	100	3
3	$Zn/CaCO_3$	500	2:30	100	5
4	$Ni/CaCO_3$	500	2:30	100	1
5	$Ni/CaCO_3$	500	2:30	100	3
6	$Ni/CaCO_3$	500	2:30	100	5
7	Zn/CaO	500	2:30	100	1
8	Zn/CaO	500	2:30	100	3
9	Zn/CaO	500	2:30	100	5

Table 3.3: Design of Experiments

Each sample of catalyst is used for three times under three different operating pressures which are respectively 1, 3 and 5 atm. The pressure is varied while the catalyst to glycerol ratio and the carbon dioxide flow rate are kept constant, to check for the effects of pressure on the gaseous products yield. The catalyst is loaded at the middle of the reactor with an amount of 5 gram. Respectively, the amount of glycerol supplied is 75 gram in 20 minutes. This corresponds to 3.75 gr/min of glycerol which is 3mL/min of glycerol. The CO_2 flow rate is set as 100mL/min.

4 RESULTS AND DISCUSSION

4.1 Catalyst Characterization

Until the beginning of November, 3 samples of the catalyst have been prepared successfully until the calcination step and sent to the Central Analytical Laboratory (CAL), UTP for BET and TEM analysis. The results for BET and TEM analysis are ready at the moment (Appendix B).

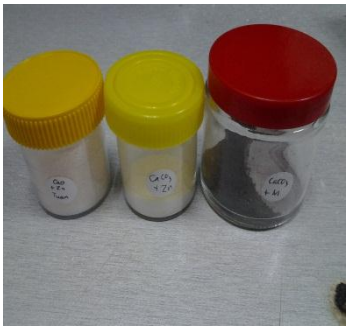

Figure 4.1: Three Catalysts Sample

The BET results are summarised below:

Type	BET Surface area (m^2/g)	Average pore size (Å)	Average pore volume (cm^3/g)
$CaCO_3$	1.9115	101.7459	0.004862
$ZnO/CaCO_3$	4.0407	127.5848	0.012888
$NiO/CaCO_3$	4.4823	131.4682	0.014732
CaO	11.5290	241.4438	0.069590
ZnO/CaO	4.6230	138.9215	0.016056

Table 4.1: BET Results

As we can see on the table above, compared to the raw $CaCO_3$ with BET surface area of 1.9115 m^2/g, the BET surface area of $ZnO/CaCO_3$ and $NiO/CaCO_3$ have been increased to 4.0407 m^2/g and 4.4823 m^2/g, respectively. At the same time, the average pore size and the average pore volume of these two catalysts exhibit a slight increment compared to the $CaCO_3$ support. Probably, this result implied the formation of a new phase by the current procedure used for the catalyst preparation.

On the other hand, the ZnO/CaO exhibits a significant decrement in terms of surface area, average pore volume and average pore size compared to the CaO support. It is reported by Grandos et al. (2007) that the transformation of CaO to $Ca(OH)_2$ is very fast. Thus, during the BET analysis, upon contacting with the moisture in the atmosphere, the surface of CaO may hydrate to become $Ca(OH)_2$. Since the hydroxide phase was generated by the hydration of CaO to $Ca(OH)_2$, the surface area of the CaO sample is higher compared to the usual size. Therefore, for the Zn/CaO sample, the presence of the Zn precursor may suppress the formation of $Ca(OH)_2$ by blocking the surface of the CaO from contacting with moisture in the atmosphere. If this was the case, then the presence of Zn has blocked the basic sites on the surface which may hinder the dry reforming reaction.

These results are supported by these TEM images:

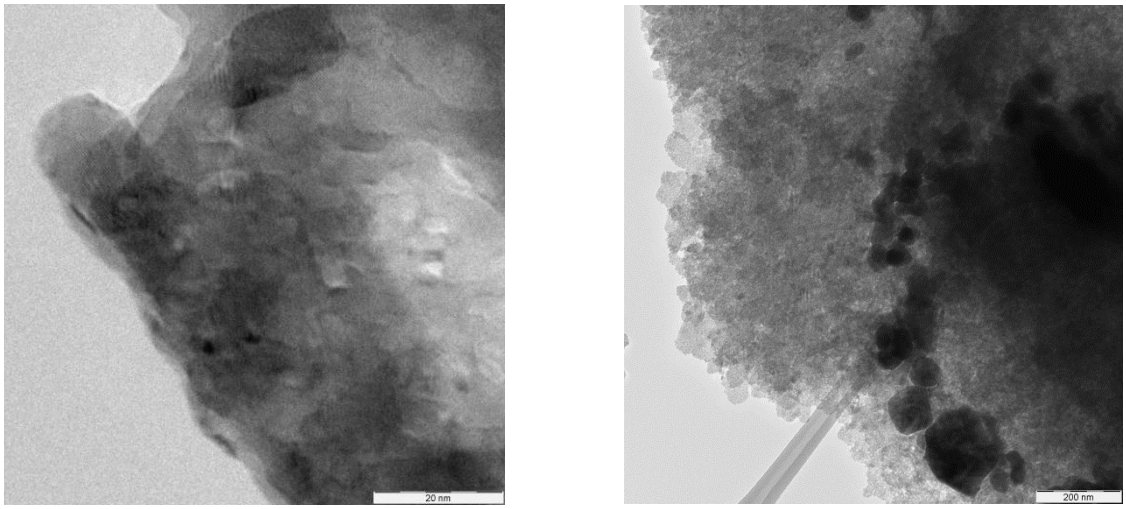

Figure 4.2: TEM images of $CaCO_3$ and $NiO/CaCO_3$ after calcination

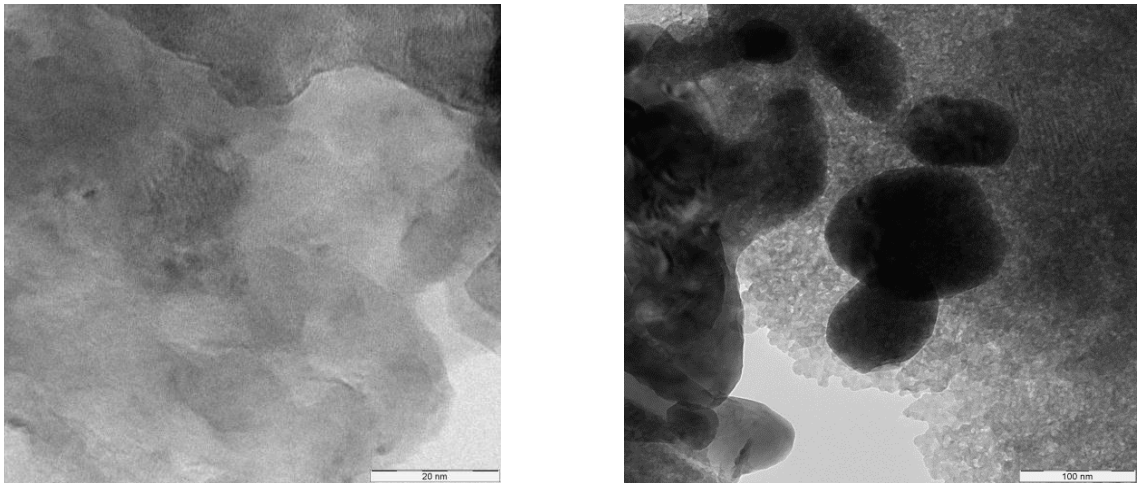

Figure 4.3: TEM images of $CaCO_3$ and $ZnO/CaCO_3$ after calcination

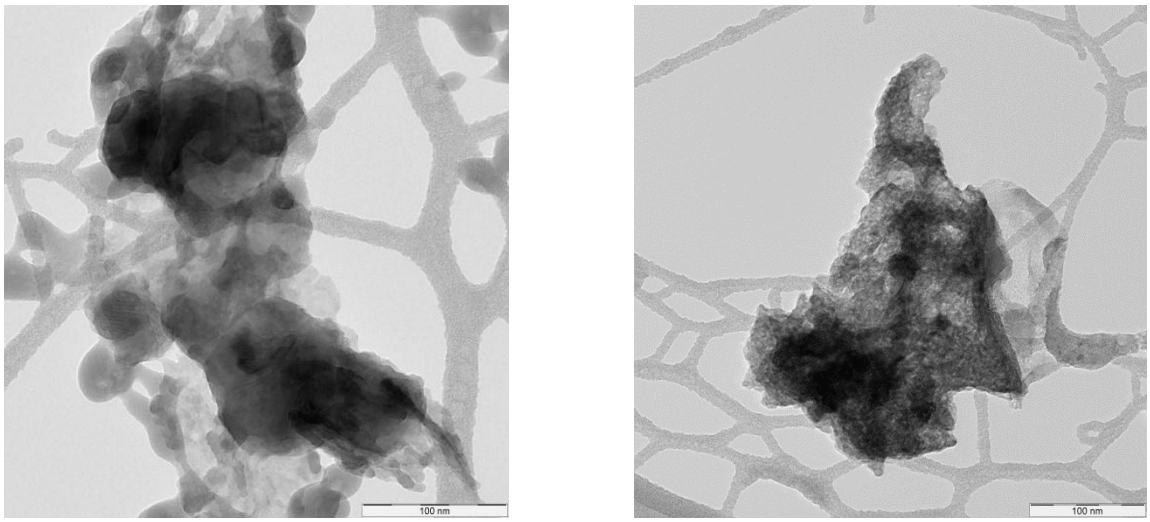

Figure 4.4: TEM images of CaO and ZnO/CaO after calcination

As can be seen on figure 4.2 and 4.3 above, the surface of $Zn/CaCO_3$ and $Ni/CaCO_3$ has been distributed with some particles of the metal precursor Zn and Ni. That indicates a new phase has been formed on the surface of the $CaCO_3$ support, which exhibits in BET results by an increment in surface area, average pore size and pore volume.

In Figure 4.4, the TEM images of CaO and Zn/ CaO after calcination have clearly shown the differences between the two surfaces. In the left figure, the $Ca(OH)_2$ formed during the hydration of CaO is distributed across the surface of the sample. While in the right figure, as Zn is blocking the surface of CaO from contacting with moisture in the atmosphere, it contributes to a decrement in surface area as well as pore size and pore volume of the catalyst sample.

4.2 Experimental Results

At the beginning of December, 9 air bags product sample have been collected based on the design of experiments. The collected air bags were sent to the Centre of Bio-fuel and Bio-Chemical Research (CBBR), UTP for Gas Chromatograph (GC) analysis.

Figure 4.5: Air Bags Product Sample

The proportion of hydrogen, carbon monoxide and unreacted carbon dioxide and hydrogen in the gaseous product was determined by a gas chromatograph (Shimadzu GC-8A) equipped with a thermal conductivity detector (TCD) and a stainless steel column packed with molecular sieve 5A using Helium as the carrier gas. The temperatures of the detector and column were maintained at 300^{o}C and 60^{o}C, respectively.

The nine air bags sample have shown similar results in term of retention time and concentration of components. Based on Shimadzu calibration reference of the same packed column using Helium as the carrier gas, we can identify the components and its respective concentration.

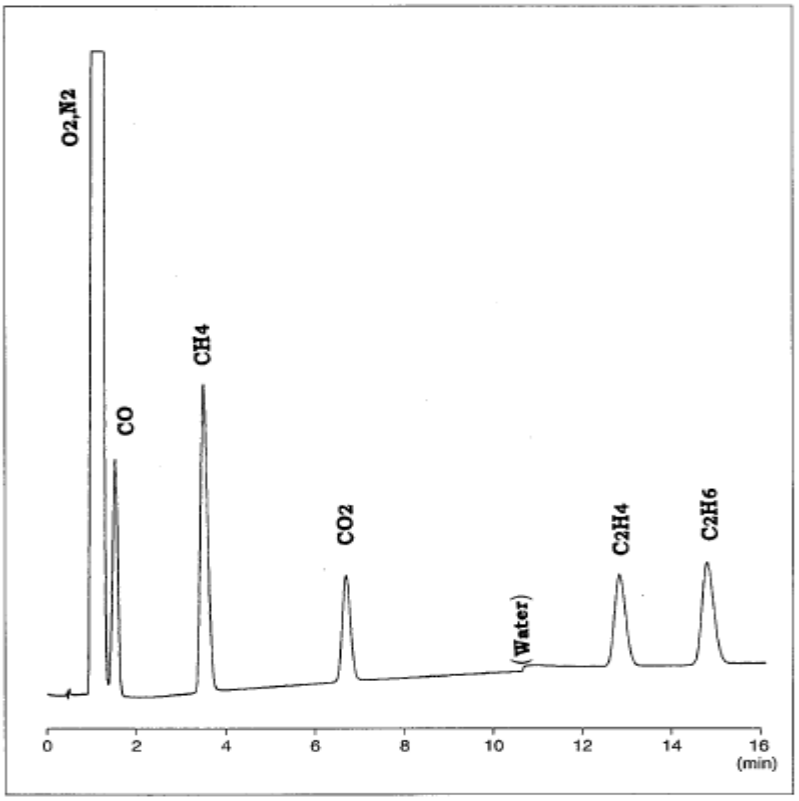

Figure 4.6: Reference calibration curve of Shimadzu GC

As we can see on the reference calibration curve above, CO and CO_2 have the retention time around 1.5 minutes and 7 minutes respectively. Moreover, according to Peter Adam (2012), the viscosity of hydrogen is the lowest compared to the other two common carrier gases Nitrogen (N_2) and Helium (He) as shown on the following figure:

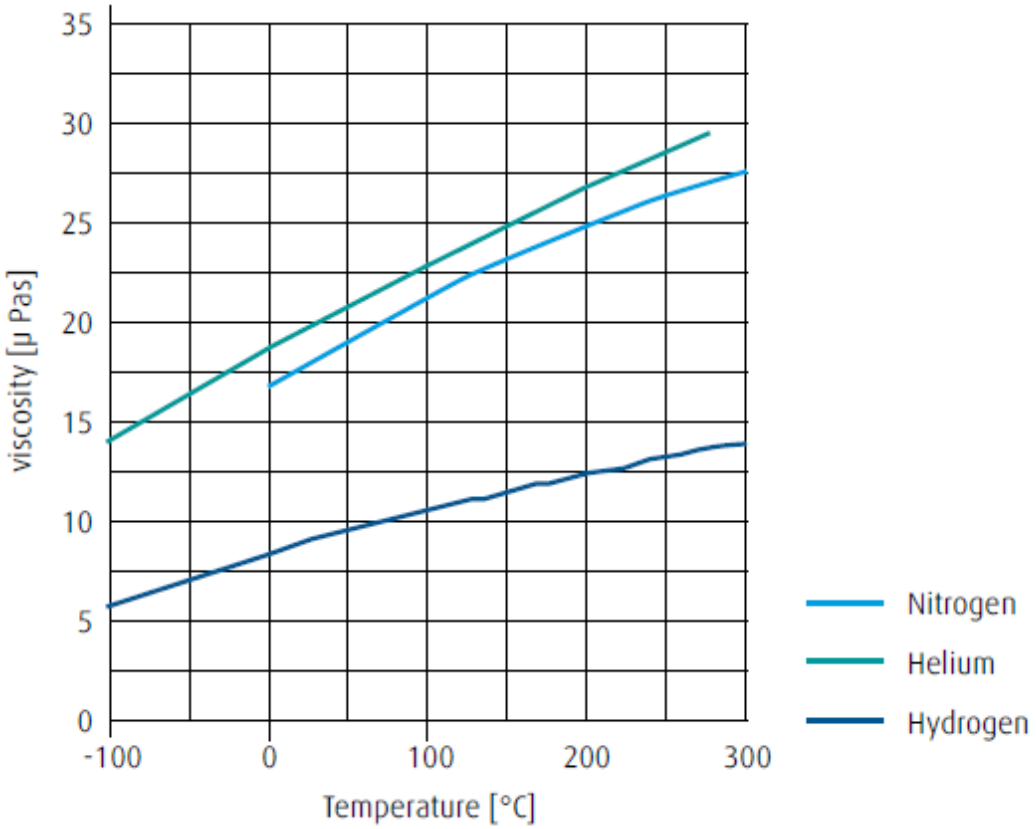

Graph 4.1: Viscosity of common carrier gases

Therefore, in our GC analysis (Appendix C), the gas that elutes faster than Nitrogen (N_2) and oxygen (O_2) (components of air which the retention time is measured at 1.245 minutes) is identified as hydrogen (H_2) with retention time of 0.871 minutes. The main objective of this project has been achieved as H_2 and CO are the two main components in the gaseous product. H_2 concentration ranges from 40 to 87% of molar concentration while CO concentration has the range of 0.36 to 7%. However, as the CO_2 peak in our results is infinitesimal, it means that the CO_2 reacted completely during the dry reforming reaction which indicates the unreacted glycerol is still in the gaseous product. Since the main product is syngas, we would rather have CO_2 in the main product than glycerol, thus, the CO_2 flow rate in the next experiment is required to be adjusted higher to completely react with glycerol.

The table below summarised the retention time of the four components we are interested in:

Components	Retention time (min)
H_2	0.859
CO	1.458
CO_2	7.079
Glycerol	9.040

Table 4.2: Retention time of main components

Relationship between types of catalyst and operating pressure towards the ratio of H_2 and CO is summarised in the following chart:

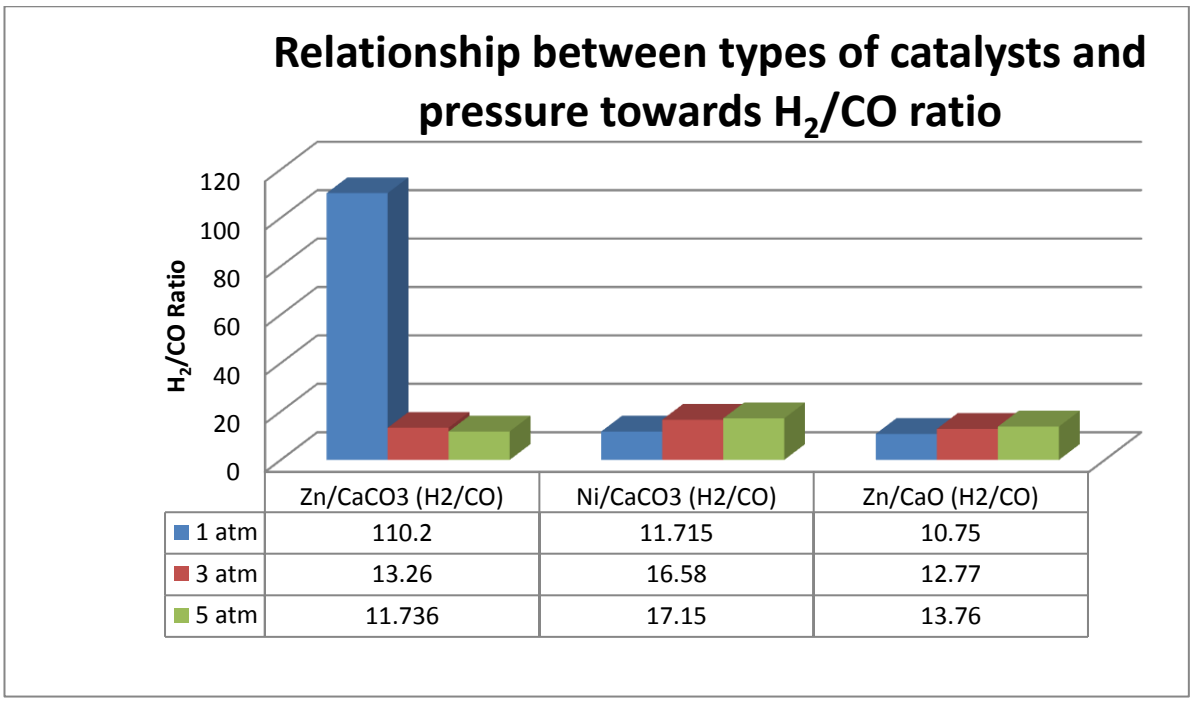

Graph 4.2: Relationship between types of catalysts and operating pressure towards H_2/CO Ratio

From the chart above, except the first H_2/CO ratio obtained from Zn/$CaCO_3$ under 1 atm, which has an exceptional value compare to the other ratios, the rest of the values are directly proportional to the operating pressures. The noticeable difference from the first value can be reasonably explained as a problem during the start-up of the experiment while the operation was not fully smooth and well-prepared. Therefore, we can conclude that as the operating pressure is increased, it enhances the H_2/CO ratio. Although the H_2/CO ratio is more than 10 even at 1 atmospheric pressure, the operating pressure can still be an important factor to control the varying amount of H_2 and CO in the syngas product composition.

5 CONCLUSIONS AND RECOMMENDATIONS

5.1 Conclusions

It is possible to complete the project within the given period. At the moment, it is proven that all of the three $CaCO_3$ and CaO based catalysts have the capability to transform glycerol into syngas via dry reforming reaction.

Many researches and commercial work have been conducted in transforming glycerol into syngas but none of them truly investigated the possibilities of using limestone (or $CaCO_3$) as the based catalyst via dry reforming. Thus, this describes how important is the study regarding limestone and dry reforming.

The results obtained from the project have shown some potential promises which would in turn create a big opportunity for Malaysia to convert glycerol into high value product syngas. The study has to continue in order to increase its potential to be commercialized as a process.

5.2 Recommendations

This FYP project has opened up several opportunities for further study. The following issues are recommended for future work in increasing the potential of transforming glycerol into syngas using limestone based catalyst:

1. The continuation of the project can be done by using real limestone in Malaysia as the based catalyst, along with the same metal precursor Zn and Ni to truly evaluate the potential of transforming glycerol into syngas using limestone based catalyst via dry reforming.

2. Steam reforming and pyrolysis reaction is encouraged to be conducted for the enhancement of conversion and selectivity as well as developing other new method and techniques in terms of operating conditions to carry out the process in bigger scales.

6 REFERENCES

1. Norhasyimi, R., Ahmad, Z.A., & Abdul, R.M., 2010, "Recent progress on innovative and potential technologies for glycerol transformation into fuel additives: A critical review", *Renewable and Sustainable Energy Reviews* **14**: 987-1000

2. Tan, B.K. 2002. *Environmental Geology of Limestone in Malaysia.* Universiti Kebangsaan Malaysia, Bangi, Malaysia

3. Adam, J.B., Pant, K.K., & Ram, B.G., 2008, "Hydrogen production from glycerol by reforming in supercritical water over Ru/Al_2O_3 catalyst", *Fuel* **97**: 2956-2960

4. Valliyapan, T., Bakhshi, N.N., & Dalai, A.K., 2008, "Pyrolysis of glycerol for the production of hydrogen or syn gas", *Bioresource Technology* **99**: 4476-4483

5. Francisco, P., Gerardo, S., & Nora, N.N., 2010, "Hydrogen and/or syngas from steam reforming of glycerol. Study of platinum catalysts", *International journal of hydrogen energy* **35**: 8912-8920

6. Fernandez, Y., Arenillas, A., Bermudez, J.M., & Menendez, J.A., 2010,"Comparative study of conventional and microwave-assisted pyrolysis, steam and dry reforming of glycerol for syngas production, using a carbonaceous catalyst", *Journal of Analytical and Applied Pyrolysis* **88**: 155–159

7. Chawalit, N., et al., 2011, "Preparation of heterogeneous catalysts from limestone for transesterification of vegetable oils- Effects of binder addition", *Journal of Industrial and Engineering Chemistry* **17**: 587-595

8. Pomonis, P. J., et al., 2005, "The I-point method for estimating the surface area of solid catalysts and the variation of C-term of the BET equation", *Catalysis Communications* **6**: 93-96

9. Francesco, P., 1998, "Supported metal catalysts preparation", *Catalysis Today* **41**: 129-137

10. Eigenberger, G. 2000. *Fixed Bed Reactors*. Ullmann's Encyclopedia of Chemical Industry, John Wiley & Sons

11. Xiaodong, W., et al., 2009, "Thermodynamic analysis of glycerol dry reforming for hydrogen and synthesis gas production", *Fuel* **88**: 2148-2153

12. Bournay, L., et al., 2005, "New heterogeneous process for biodiesel production: A way to improve the quality and the value of the crude glycerine produced by biodiesel plants", *Catalysis Today* **106**: 190-192

13. Lopez Granados, M., et al., 2007, "Biodiesel from sunflower oil by using activated calcium oxide", *Applied Catalysis B: Environmental* **73**: 317-326

14. Peter Adam, 2012, Application notes for Speciality Gases. Hydrogen as an alternative to Helium for Gas Chromatography, The Linde Group.

15. Shimadzu Application News, 2010, www.ssi.shimadzu.com

7 APPENDICES

APPENDIX A:

COMPLETE CONFIGURATION OF REACTOR

APPENDIX B:

BET ANALYSIS

micromeritics

Full Report Set

ASAP 2020 V3.04 H | Unit 1 | Serial #: 1161 | Page 1

Sample: 000-618 J134/SAP/11/12 CaCo3
Operator: Omar
Submitter: Ahmad Fikri
File: C:\2020\DATA\NOVEMB~1\000-618.SMP

Started: 11/2/2012 9:55:31AM
Completed: 11/2/2012 2:17:50PM
Report Time: 11/7/2012 10:20:25AM
Sample Mass: 0.2976 g
Cold Free Space: 83.3558 cm³
Low Pressure Dose: None

Analysis Adsorptive: N2
Analysis Bath Temp.: -195.860 °C
Thermal Correction: No
Warm Free Space: 27.7821 cm³ Measured
Equilibration Interval: 10 s
Automatic Degas: Yes

Summary Report

Surface Area

Single point surface area at P/Po = 0.249833403: 1.5726 m²/g

BET Surface Area: 1.9115 m²/g

Langmuir Surface Area: 3.6144 m²/g

t-Plot External Surface Area: 3.1241 m²/g

BJH Adsorption cumulative surface area of pores between 17.000 Å and 3000.000 Å width: 2.678 m²/g

BJH Desorption cumulative surface area of pores between 17.000 Å and 3000.000 Å width: 2.5535 m²/g

Pore Volume

Single point adsorption total pore volume of pores less than 1417.769 Å width at P/Po = 0.986159447: 0.004862 cm³/g

Single point desorption total pore volume of pores less than 795.467 Å width at P/Po = 0.975047566: 0.004296 cm³/g

t-Plot micropore volume: -0.000759 cm³/g

BJH Adsorption cumulative volume of pores between 17.000 Å and 3000.000 Å width: 0.005801 cm³/g

BJH Desorption cumulative volume of pores between 17.000 Å and 3000.000 Å width: 0.005976 cm³/g

Pore Size

Adsorption average pore width (4V/A by BET): 101.7459 Å

Desorption average pore width (4V/A by BET): 89.9084 Å

BJH Adsorption average pore width (4V/A): 86.641 Å

BJH Desorption average pore width (4V/A): 93.618 Å

Figure B.1: BET analysis of $CaCO_3$

Full Report Set

TriStar II 3020 V1.04 (V1.04) Unit 1 Port 2 Serial #: 844 Page 1

Sample: 000-095 J141/SAP/11/12 CaCo3+ZnO
Operator: Omar
Submitter: Do Minh
File: C:\WIN3020\DATA\000-095.SMP

Started: 7/11/2012 5:38:38AM
Completed: 7/11/2012 11:05:05AM
Report Time: 8/11/2012 9:48:53PM
Warm Free Space: 20.7736 cm³ Measured
Equilibration Interval: 10 s
Sample Density: 1.000 g/cm³

Analysis Adsorptive: N2
Analysis Bath Temp.: -195.800 °C
Sample Mass: 0.3008 g
Cold Free Space: 58.4857 cm³ Measured
Low Pressure Dose: None
Automatic Degas: Yes

Sample Prep: Stage	Temperature (°C)	Ramp Rate (°C/min)	Time (min)
1	90	10	30
2	250	10	240

Summary Report

Surface Area

Single point surface area at p/p° = 0.299456523: 3.4528 m²/g
BET Surface Area: 4.0407 m²/g
Langmuir Surface Area: 7.5922 m²/g
t-Plot External Surface Area: 6.6923 m²/g
BJH Adsorption cumulative surface area of pores between 17.000 Å and 3000.000 Å diameter: 3.969 m²/g
BJH Desorption cumulative surface area of pores between 17.000 Å and 3000.000 Å diameter: 4.7474 m²/g

Pore Volume

Single point adsorption total pore volume of pores less than 2983.750 Å diameter at p/p° = 0.993491904: 0.012888 cm³/g
t-Plot micropore volume: -0.001597 cm³/g
BJH Adsorption cumulative volume of pores between 17.000 Å and 3000.000 Å diameter: 0.012242 cm³/g
BJH Desorption cumulative volume of pores between 17.000 Å and 3000.000 Å diameter: 0.016675 cm³/g

Pore Size

Adsorption average pore width (4V/A by BET): 127.5848 Å
BJH Adsorption average pore diameter (4V/A): 123.387 Å
BJH Desorption average pore diameter (4V/A): 140.495 Å

Figure B.2: BET analysis of $ZnO/CaCO_3$

Full Report Set

TriStar II 3020 V1.04 (V1.04) Unit 1 Port 3 Serial #: 844 Page 1

Sample: 000-096 J141/SAP/11/12 CaCo3+NiO
Operator: Omar
Submitter: Do Minh
File: C:\WIN3020\DATA\000-096.SMP

Started: 7/11/2012 5:38:38AM
Completed: 7/11/2012 11:05:05AM
Report Time: 8/11/2012 9:48:54PM
Warm Free Space: 20.7132 cm³ Measured
Equilibration Interval: 10 s
Sample Density: 1.000 g/cm³

Analysis Adsorptive: N2
Analysis Bath Temp.: -195.800 °C
Sample Mass: 0.2979 g
Cold Free Space: 58.1568 cm³ Measured
Low Pressure Dose: None
Automatic Degas: Yes

Sample Prep: Stage	Temperature (°C)	Ramp Rate (°C/min)	Time (min)
1	90	10	30
2	250	10	240

Summary Report

Surface Area

Single point surface area at p/p° = 0.299469161: 3.6018 m²/g

BET Surface Area: 4.4823 m²/g

Langmuir Surface Area: 9.5088 m²/g

t-Plot External Surface Area: 7.7373 m²/g

BJH Adsorption cumulative surface area of pores between 17.000 Å and 3000.000 Å diameter: 4.546 m²/g

BJH Desorption cumulative surface area of pores between 17.000 Å and 3000.000 Å diameter: 4.7346 m²/g

Pore Volume

Single point adsorption total pore volume of pores less than 2943.274 Å diameter at p/p° = 0.993401376: 0.014732 cm³/g

t-Plot micropore volume: -0.002062 cm³/g

BJH Adsorption cumulative volume of pores between 17.000 Å and 3000.000 Å diameter: 0.014091 cm³/g

BJH Desorption cumulative volume of pores between 17.000 Å and 3000.000 Å diameter: 0.018522 cm³/g

Pore Size

Adsorption average pore width (4V/A by BET): 131.4682 Å

BJH Adsorption average pore diameter (4V/A): 123.997 Å

BJH Desorption average pore diameter (4V/A): 156.482 Å

Figure B.3: BET analysis of $NiO/CaCO_3$

micromeritics

Full Report Set

ASAP 2020 V3.04 H | Unit 1 | Serial #: 1161 | Page 1

Sample: 000-621 J134/SAP/11/12 CaO
Operator: Omar
Submitter: Ahmad Fikri
File: C:\2020\DATA\NOVEMB~1\000-621.SMP

Started: 11/6/2012 9:25:57 AM
Completed: 11/6/2012 3:06:21 PM
Report Time: 11/7/2012 10:20:28 AM
Sample Mass: 0.1670 g
Cold Free Space: 84.9591 cm³
Low Pressure Dose: None

Analysis Adsorptive: N2
Analysis Bath Temp.: -195.829 °C
Thermal Correction: No
Warm Free Space: 28.1548 cm³ Measured
Equilibration Interval: 10 s
Automatic Degas: Yes

Summary Report

Surface Area

Single point surface area at P/Po = 0.249902716: 10.6922 m²/g

BET Surface Area: 11.5290 m²/g

Langmuir Surface Area: 17.7556 m²/g

t-Plot External Surface Area: 13.4719 m²/g

BJH Adsorption cumulative surface area of pores between 17.000 Å and 3000.000 Å width: 12.702 m²/g

BJH Desorption cumulative surface area of pores between 17.000 Å and 3000.000 Å width: 13.7474 m²/g

Pore Volume

Single point adsorption total pore volume of pores less than 1366.148 Å width at P/Po = 0.985627284: 0.069590 cm³/g

Single point desorption total pore volume of pores less than 971.853 Å width at P/Po = 0.979664844: 0.081176 cm³/g

t-Plot micropore volume: -0.001205 cm³/g

BJH Adsorption cumulative volume of pores between 17.000 Å and 3000.000 Å width: 0.093038 cm³/g

BJH Desorption cumulative volume of pores between 17.000 Å and 3000.000 Å width: 0.092705 cm³/g

Pore Size

Adsorption average pore width (4V/A by BET): 241.4438 Å

Desorption average pore width (4V/A by BET): 281.6409 Å

BJH Adsorption average pore width (4V/A): 292.978 Å

BJH Desorption average pore width (4V/A): 269.738 Å

Figure B.4: BET analysis of CaO

Full Report Set

TriStar II 3020 V1.04 (V1.04) Unit 1 Port 1 Serial #: 844 Page 1

Sample: 000-094 J141/SAP/11/12 CaO+ZnO
Operator: Omar
Submitter: Do Minh
File: C:\WIN3020\DATA\000-094.SMP

Started: 7/11/2012 5:38:38AM
Completed: 7/11/2012 11:05:05AM
Report Time: 8/11/2012 9:48:53PM
Warm Free Space: 20.2852 cm³ Measured
Equilibration Interval: 10 s
Sample Density: 1.000 g/cm³

Analysis Adsorptive: N2
Analysis Bath Temp.: -195.800 °C
Sample Mass: 0.3004 g
Cold Free Space: 56.7143 cm³ Measured
Low Pressure Dose: None
Automatic Degas: Yes

Sample Prep: Stage	Temperature (°C)	Ramp Rate (°C/min)	Time (min)
1	90	10	30
2	250	10	240

Summary Report

Surface Area

Single point surface area at p/p° = 0.299481491: 4.0912 m²/g

BET Surface Area: 4.6230 m²/g

Langmuir Surface Area: 8.2006 m²/g

t-Plot External Surface Area: 7.2532 m²/g

BJH Adsorption cumulative surface area of pores between 17.000 Å and 3000.000 Å diameter: 4.630 m²/g

Pore Volume

Single point adsorption total pore volume of pores less than 3058.183 Å diameter at p/p° = 0.993652066: 0.016056 cm³/g

t-Plot micropore volume: -0.001554 cm³/g

BJH Desorption cumulative volume of pores between 17.000 Å and 3000.000 Å diameter: 0.019626 cm³/g

Pore Size

Adsorption average pore width (4V/A by BET): 138.9215 Å

BJH Adsorption average pore diameter (4V/A): 132.277 Å

BJH Desorption average pore diameter (4V/A): 144.319 Å

Figure B.5: BET analysis of ZnO/CaO

APPENDIX C:

GC ANALYSIS

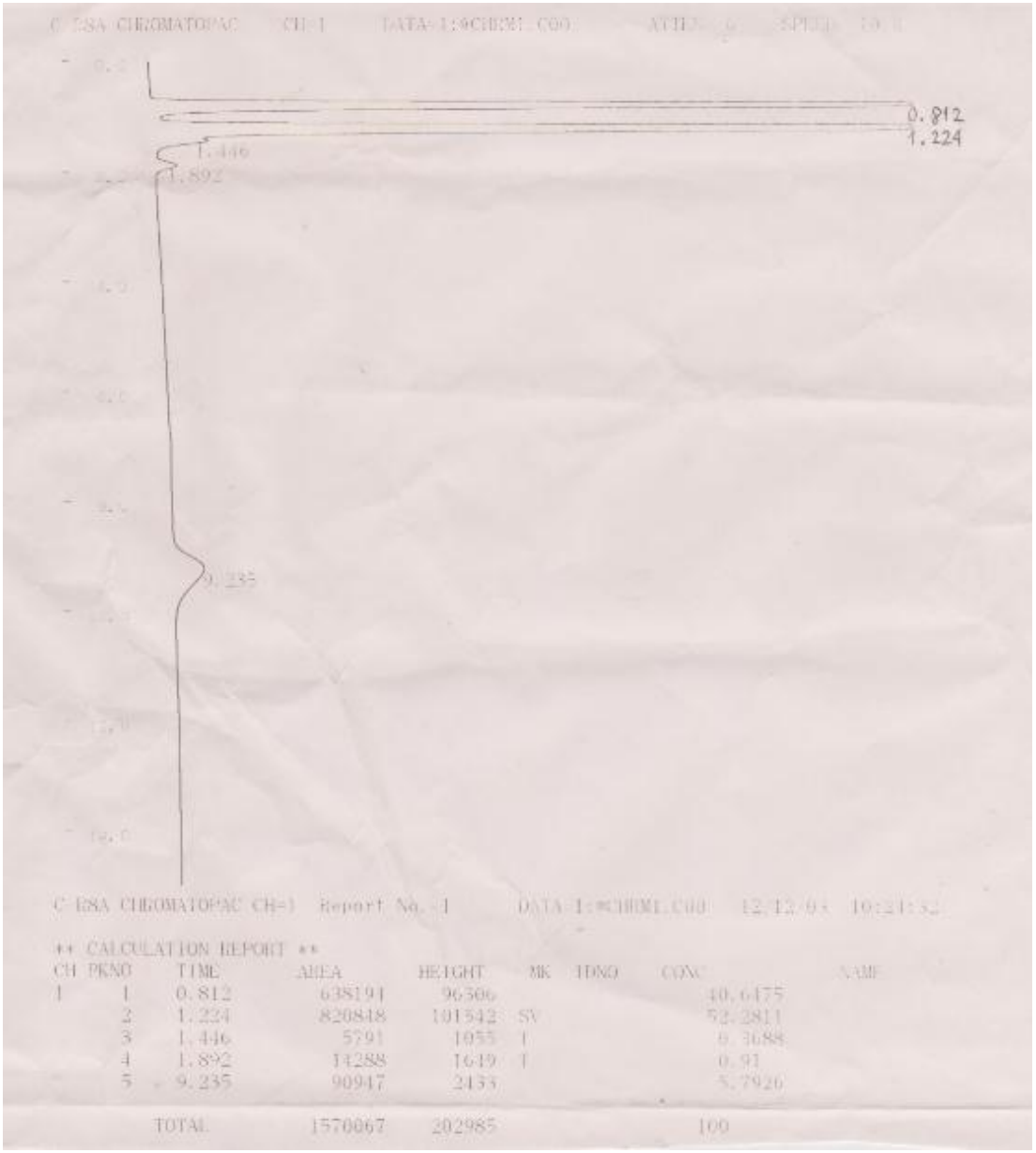

C-18A CHROMATOPAC CH=1 Report No. 1 DATA 1:¥CHROM1.C00 12.12.03 10:21:32

** CALCULATION REPORT **

CH	PKNO	TIME	AREA	HEIGHT	MK	IDNO	CONC	NAME
1	1	0.812	638191	96306			40.6475	
	2	1.224	820848	101542	SV		52.2811	
	3	1.446	5791	1055	T		0.3688	
	4	1.892	14288	1649	T		0.91	
	5	9.235	90947	2433			5.7926	
		TOTAL	1570067	202985			100	

Figure C.1: GC analysis of air bags using catalyst Zn/$CaCO_3$ at 1 atm

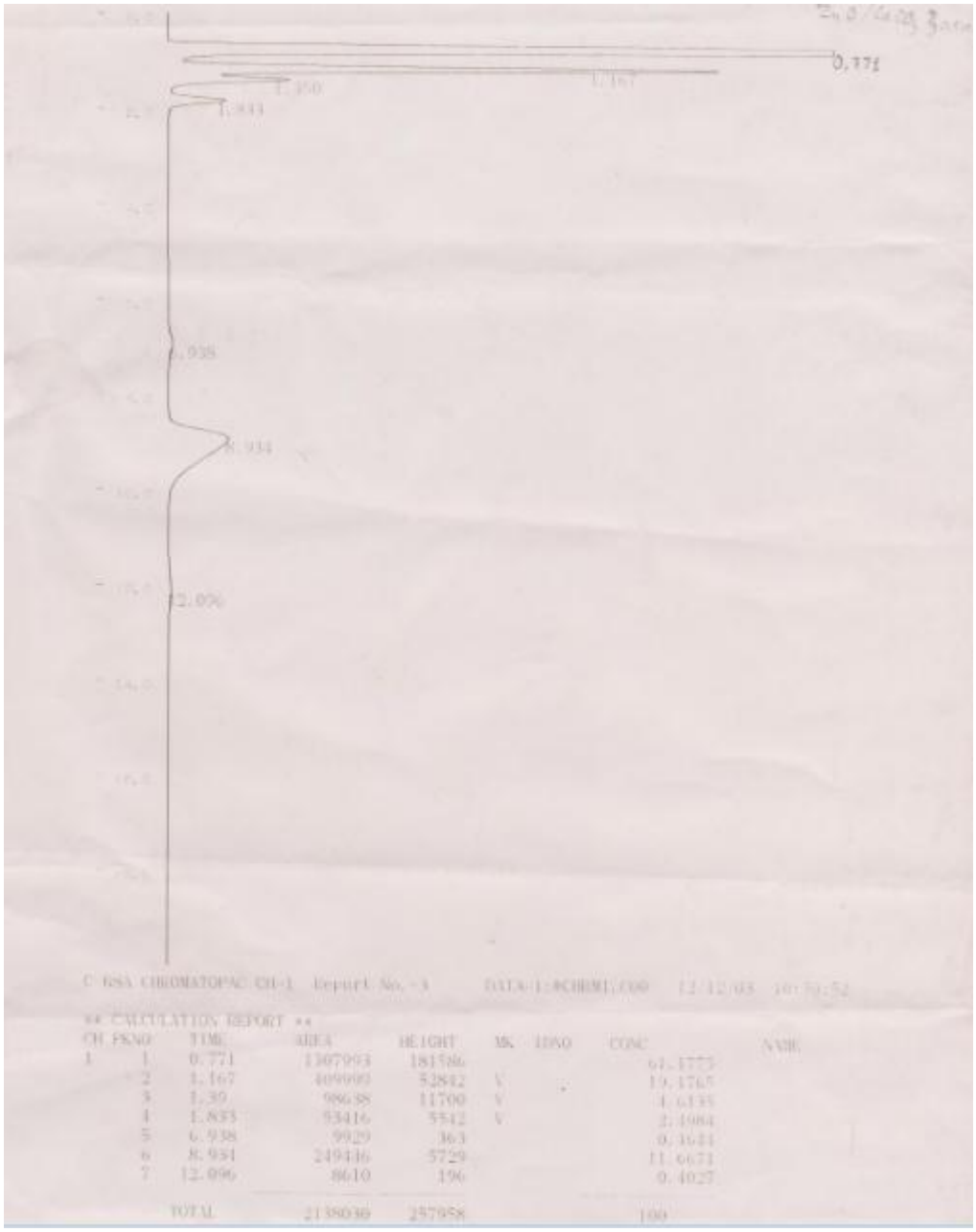

Figure C.2: GC analysis of air bags using catalyst Zn/$CaCO_3$ at 3 atm

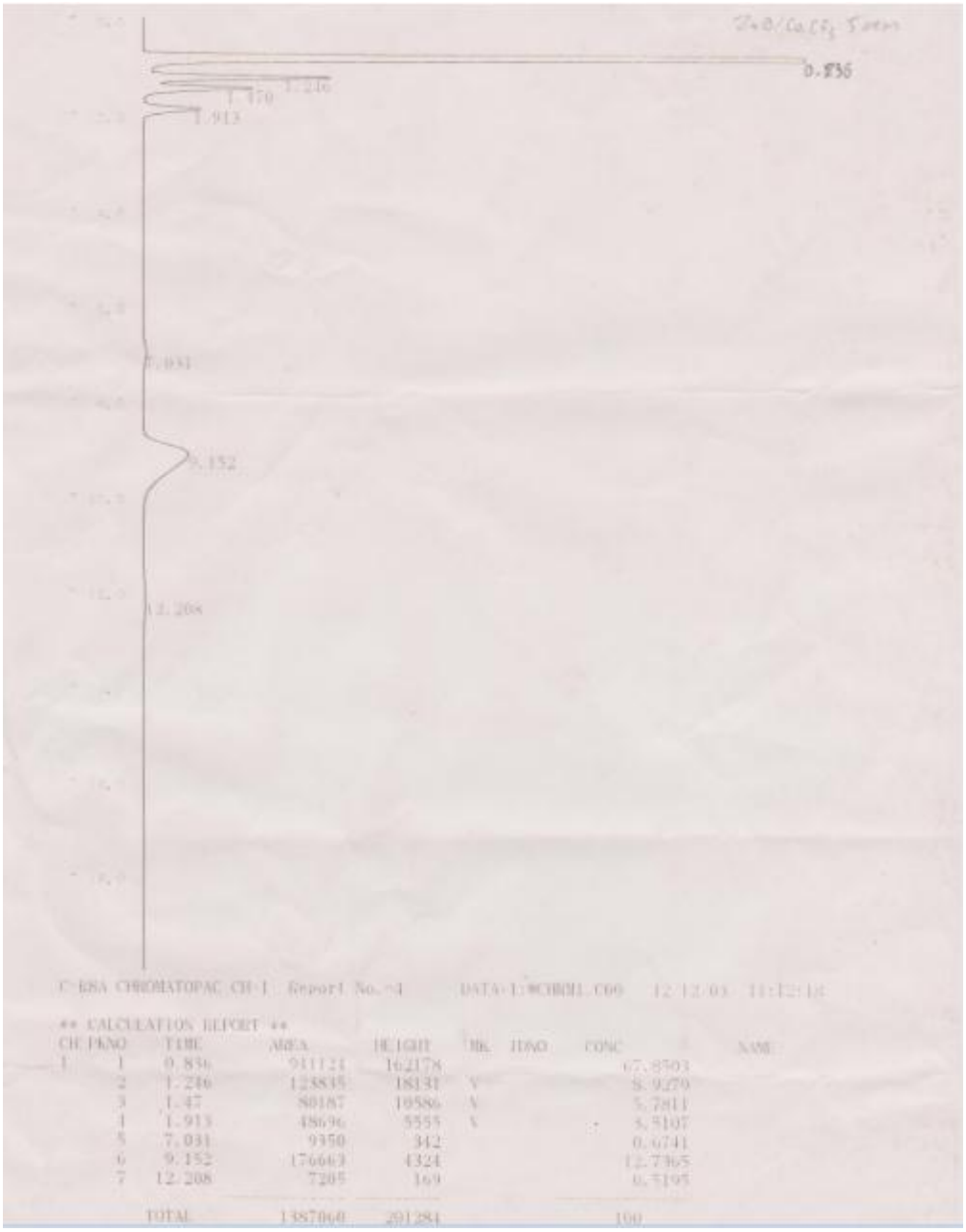

Figure C.3: GC analysis of air bags using catalyst Zn/$CaCO_3$ at 5 atm

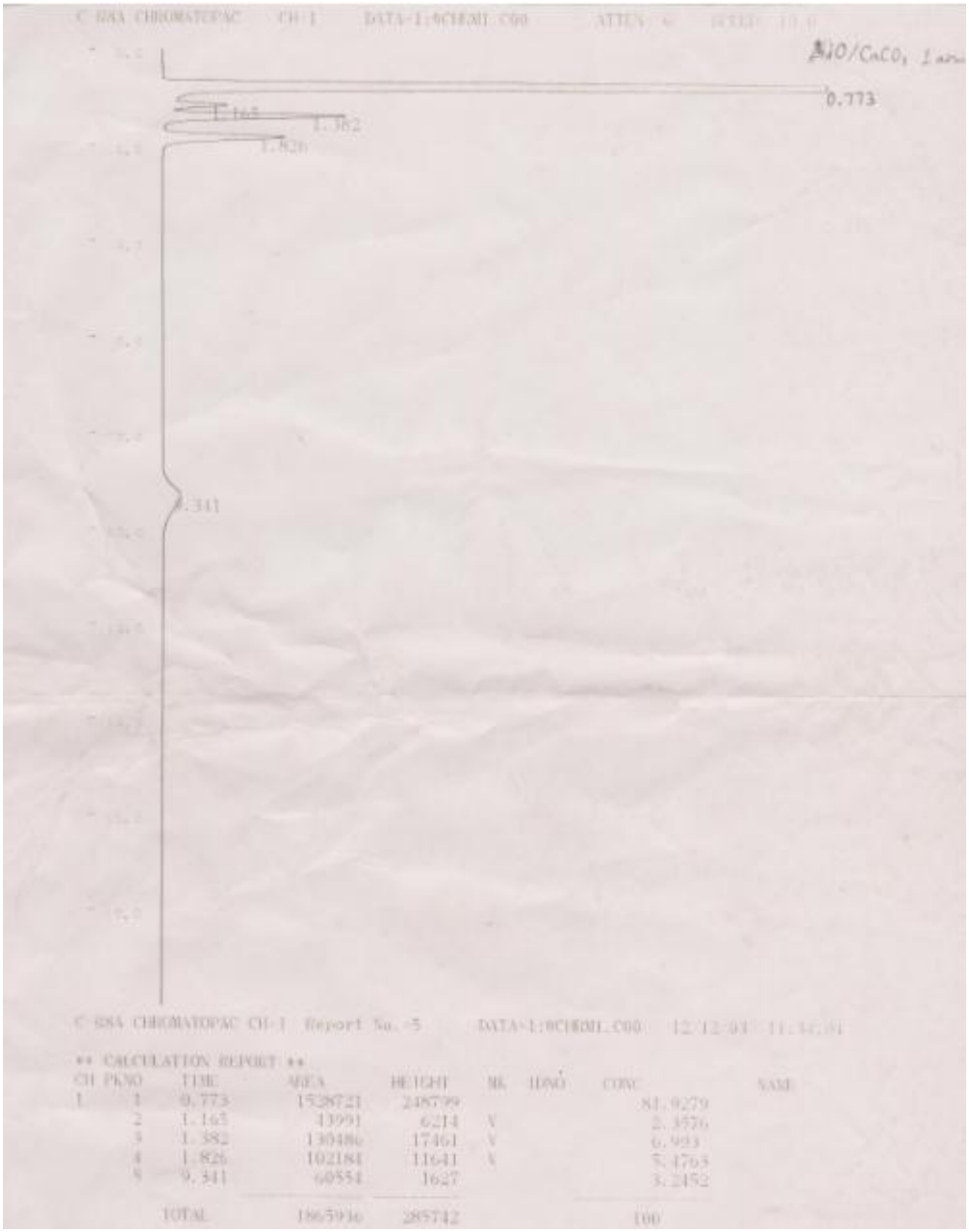

Figure C.4: GC analysis of air bags using catalyst Ni/$CaCO_3$ at 1 atm

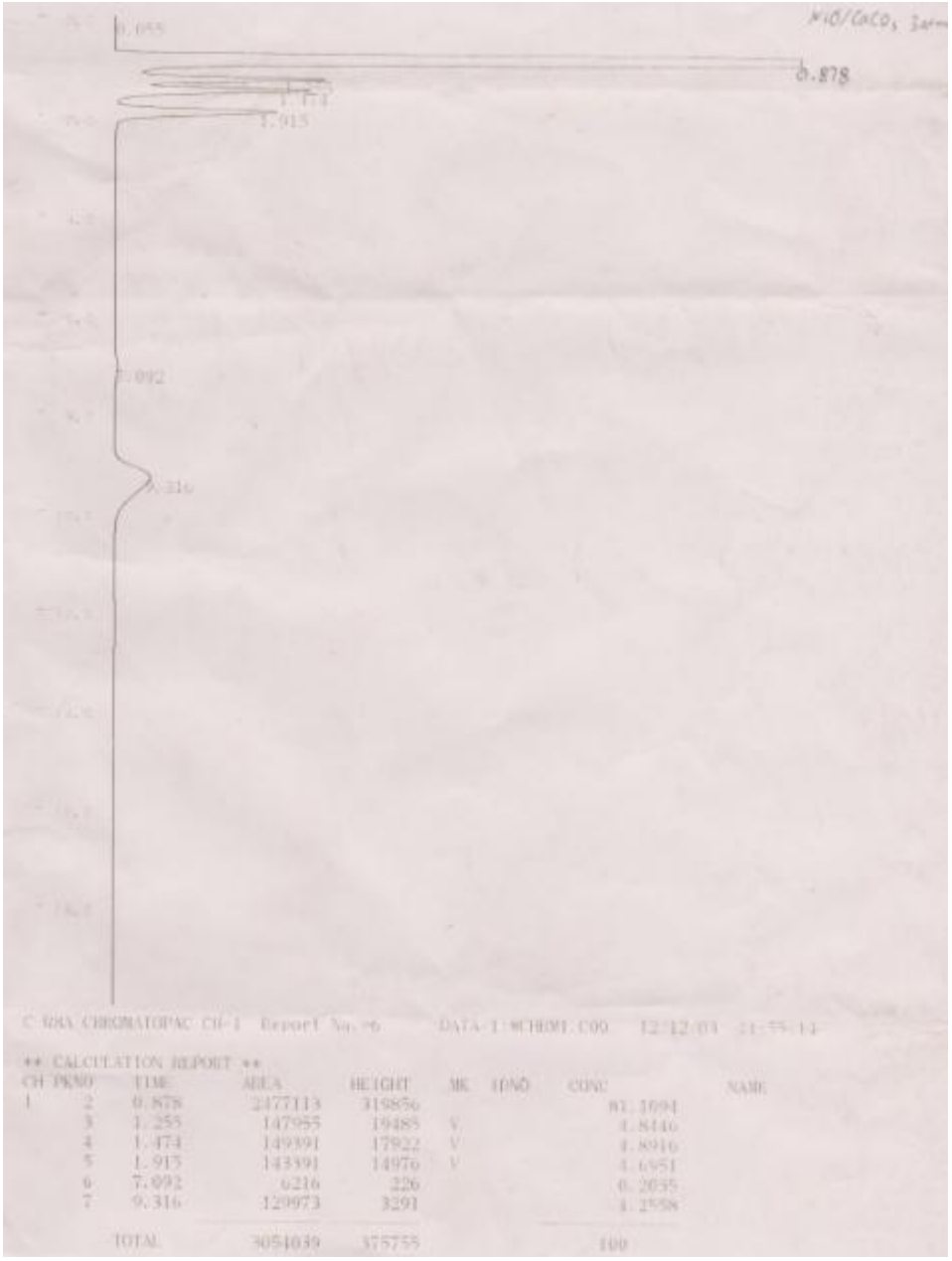

Figure C.5: GC analysis of air bags using catalyst Ni/$CaCO_3$ at 3 atm

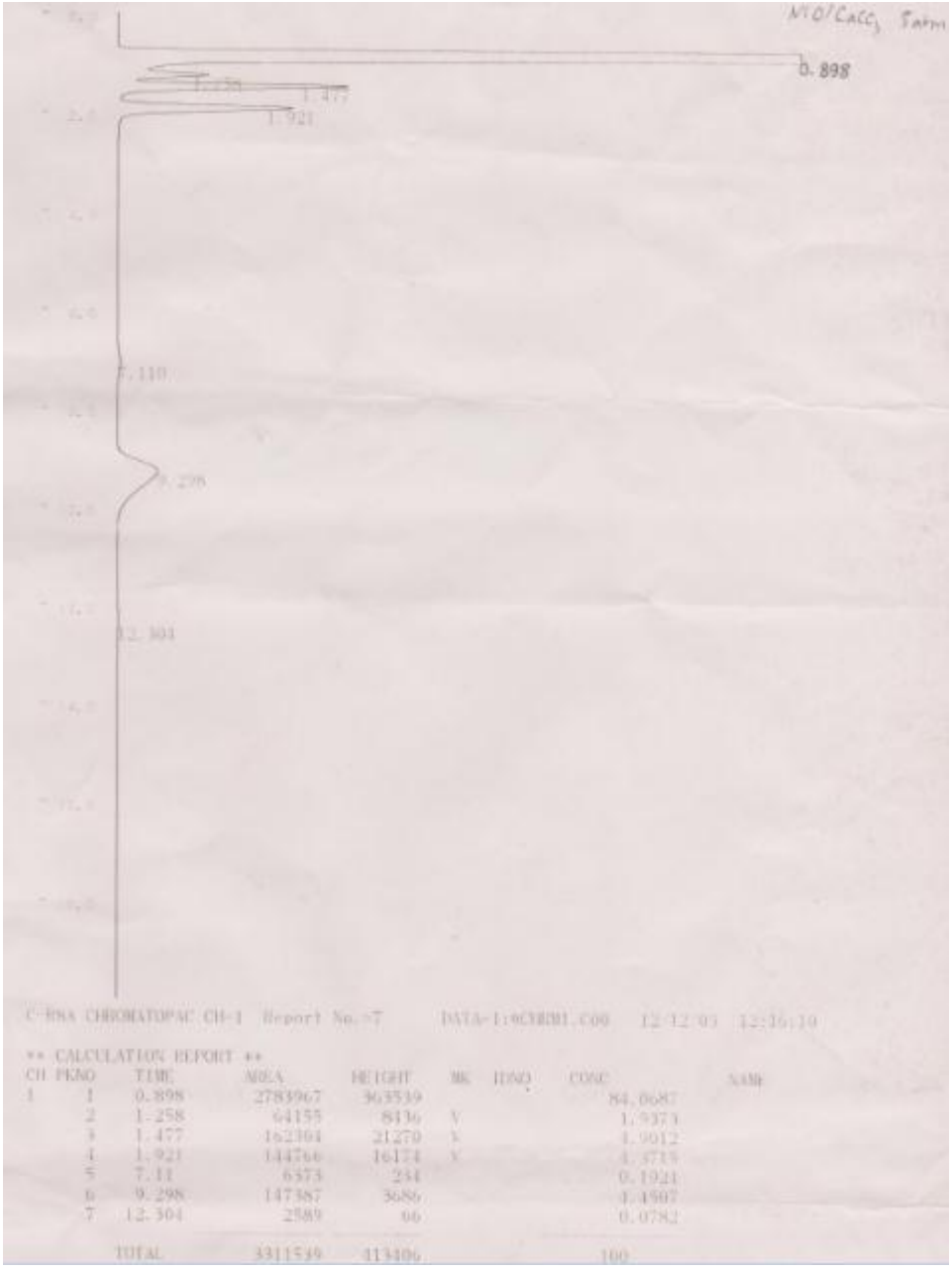

Figure C.6: GC analysis of air bags using catalyst Ni/$CaCO_3$ at 5 atm

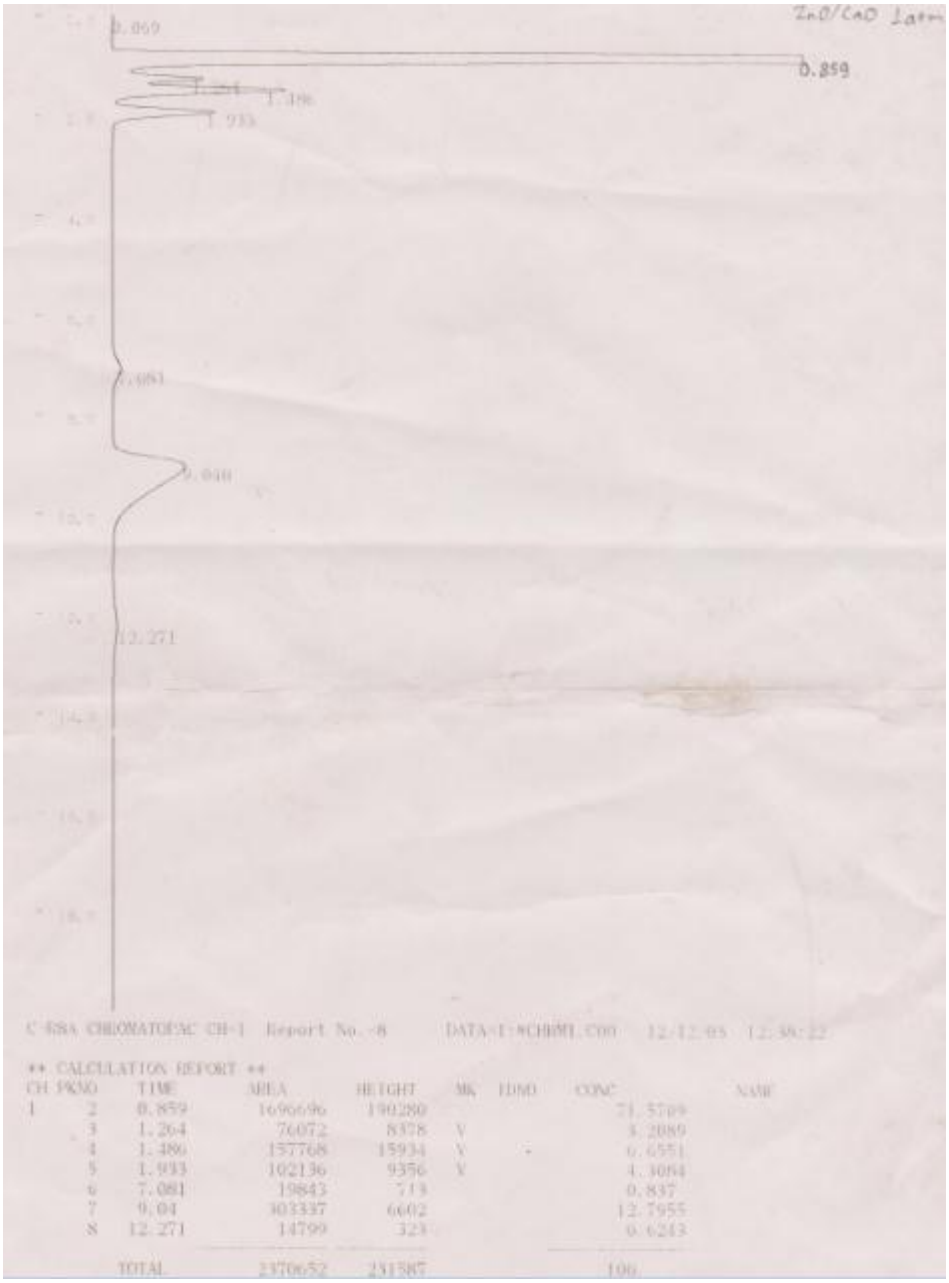

Figure C.7: GC analysis of air bags using catalyst Zn/CaO at 1 atm

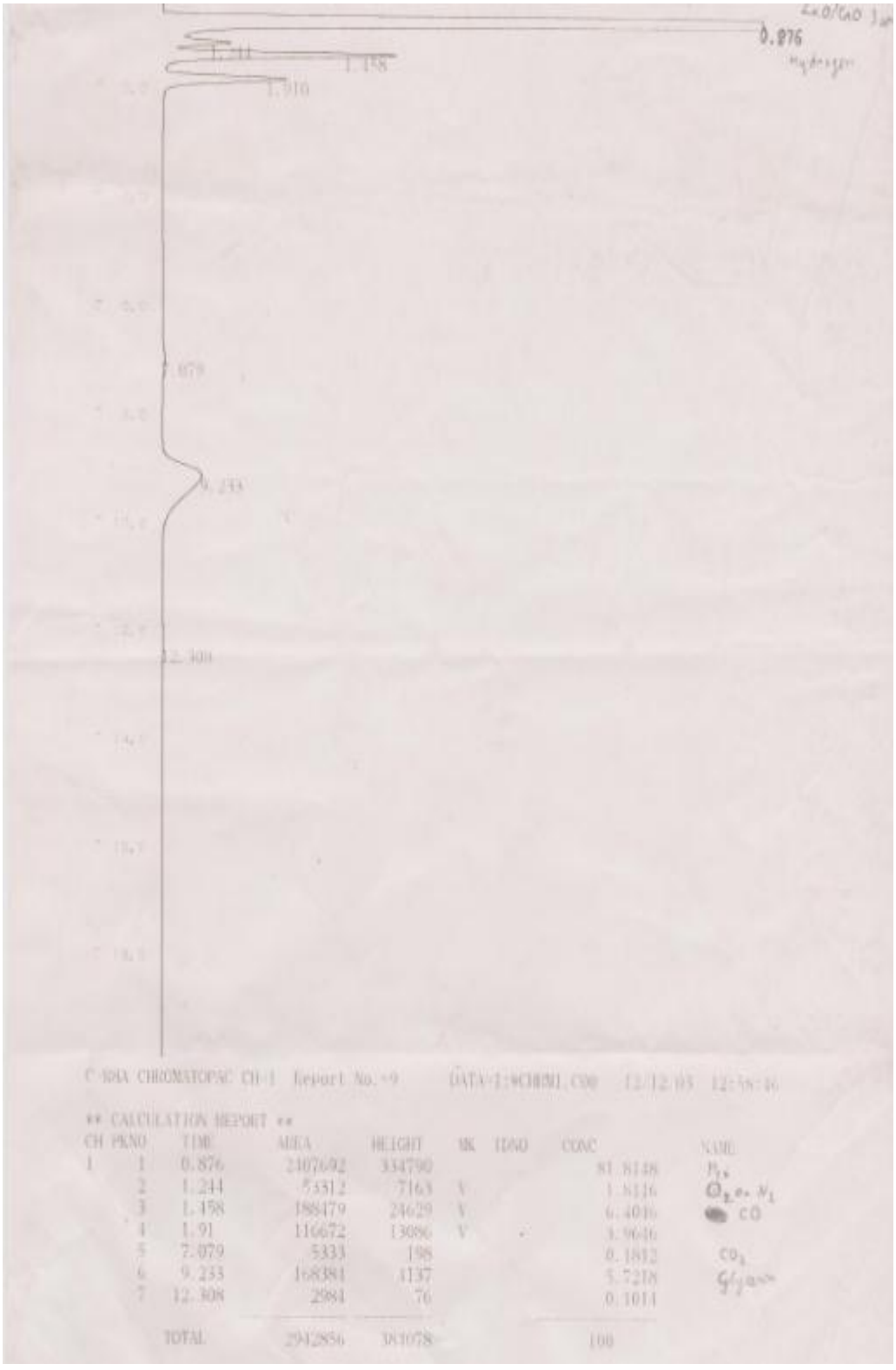

Figure C.8: GC analysis of air bags using catalyst Zn/CaO at 3 atm

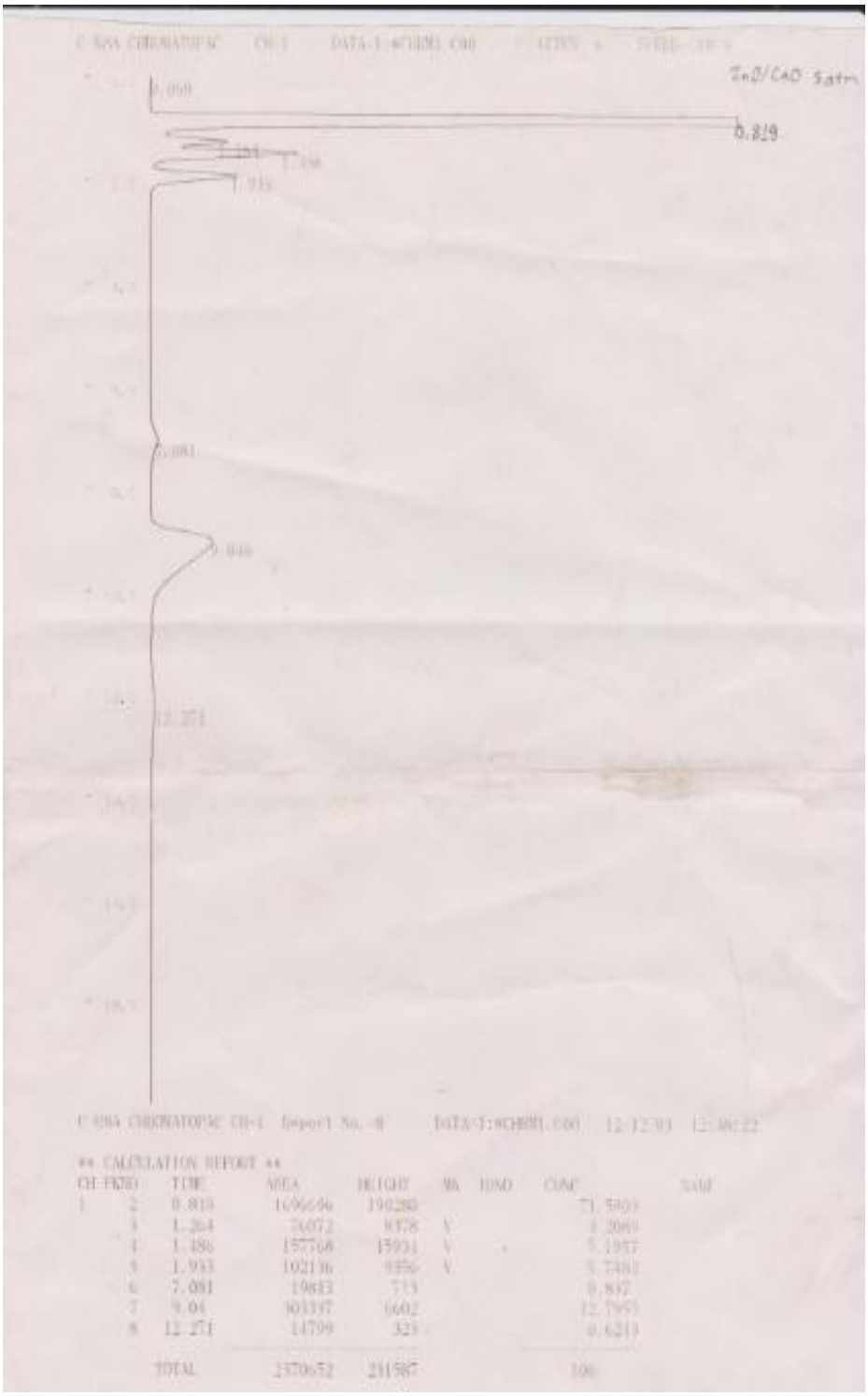

Figure C.9: GC analysis of air bags using catalyst Zn/CaO at 5 atm